

**55<sup>th</sup>** Heyrovský Discussions &  
**13<sup>th</sup>** International Zdravko Stoykov  
Symposium on Electrochemical  
Impedance Analysis

Book of Abstracts



**Castle Třešť** (Czech Republic)  
**June 9-13, 2024**

## Sponsors



55<sup>th</sup> Heyrovsky Discussion and 13<sup>th</sup> International Zdravko Stoynov Symposium  
on Electrochemical Impedance Analysis  
Castle Třešť (Czech Republic) June 9-13, 2024.



© J. Heyrovský Institute of Physical Chemistry, v.v.i, 2024  
Academy of Sciences of the Czech Republic  
Dolejškova 3, 182 23 Praha 8, Czech Republic

Edited by Jana Kocábová, Viliam Kolivoška  
72 pages – Number of copies: 50

ISBN 978-80-87351-67-3

## COMMITTEES

### CONFERENCE CHAIR

Magdaléna Hromadová, J. Heyrovský Institute of Physical Chemistry, CZ

### CONFERENCE CO-CHAIR

Romana Sokolová, J. Heyrovský Institute of Physical Chemistry, CZ

### Organizing Committee:

- Lucie Dostálková: J. Heyrovský Institute of Physical Chemistry, CZ  
*lucie.dostalkova@jh-inst.cas.cz*
- Magdaléna Hromadová: J. Heyrovský Institute of Physical Chemistry, CZ  
*magdalena.hromadova@jh-inst.cas.cz*
- Jana Kocábová: J. Heyrovský Institute of Physical Chemistry, CZ  
*jana.kocabova@jh-inst.cas.cz*
- Viliam Kolivoška: J. Heyrovský Institute of Physical Chemistry, CZ  
*viliam.kolivoska@jh-inst.cas.cz*
- Romana Sokolová: J. Heyrovský Institute of Physical Chemistry, CZ  
*romana.sokolova@jh-inst.cas.cz*

### Scientific Committee:

- **Miran Gaberšček**: National Institute of Chemistry; University of Ljubljana, SLOVENIA  
*miran.gaberscek@ki.si*
- **Magdaléna Hromadová**: J. Heyrovský Institute of Physical Chemistry, CZECH REPUBLIC  
*magdalena.hromadova@jh-inst.cas.cz*
- **Rafał Jurczakowski**: Faculty of Chemistry, University of Warsaw, POLAND *rafjur@chem.uw.edu.pl*
- **Gyöző G. Láng**: Institute of Chemistry, Eötvös Loránd University, HUNGARY  
*gyozo.lang@ttk.elte.hu*
- **X. Ramón Nóvoa Rodríguez**: School of Industrial Engineering, University of Vigo, SPAIN  
*rnovoa@uvigo.gal*
- **Tamás Pajkóssy**: Institute of Materials and Environmental Chemistry, Research Centre for Natural Sciences, HUNGARY  
*pajkossy.tamas@ttk.hu, pajkossy.tamas@ttk.mta.hu*
- **Werner Strunz**: Zahner-Elektrik GmbH & Co. KG, GERMANY  
*Werner.Strunz@zahner.de*
- **Daria Vladikova**: Institute of Electrochemistry and Energy Systems, Bulgarian Academy of Sciences; Institute for Sustainable Transition and Development, Trakia University, BULGARIA  
*d.vladikova@iees.bas.bg*

# TABLE OF CONTENTS

PROGRAM .....	4
ORAL PRESENTATIONS .....	10
POSTER PRESENTATIONS .....	52
LIST OF PARTICIPANTS.....	58
AUTHOR INDEX .....	61

## Appendix:

J-D-K-D quartet

Gothic castle Lipnice, Eavesdropping National Monument – Mouth of the truth,  
Bretschneider's ear

History of the Downtown of Havlíčkův Brod and the Brewery Rebel

Jaroslav Heyrovský

55 years of Heyrovský Discussion Meetings

History of the Castle and of the Town Třešť

## Sunday, June 9

- 10:00 Registration in **the entrance hall of the J. Heyrovský Institute**, light refreshment, possibility to leave the luggage and walk in the town
- 15:00 Departure of a special bus from the J. Heyrovský Institute (Dolejškova 3, Prague 8 – Kobylisy)
- 17:30 Arrival, registration at the Castle Třešť
- 18:30 Welcome aperitif
- 19:00 Dinner

## Monday, June 10 – morning

from  
7:00 Breakfast

8:30

### Opening of the 55th Heyrovský Discussions & 13th International Zdravko Stoynov Symposium on ELECTROCHEMICAL IMPEDANCE ANALYSIS

**Magdalena Hromadová**, past-chair  
of the ISE Division 6 Molecular Electrochemistry

**Daria Vladikova**,  
member of the EIA Scientific Committee

*Organizers* Magdaléna Hromadová  
Romana Sokolová

Topic: **Zdravko Stoynov Memorial Medal lecture**

<i>Time</i>	<i>Chairman</i>	<i>Speaker</i>		<i>Title of presentation</i>
9:00 to 10:00	Daria Vladikova	<b>Tamás Pajkóssy</b>	HU	Analysis of Quasi-Reversible CVs and dEIS Data: Transformation to Potential-Program Independent Forms.  <i>(Plenary lecture)</i>

10:00 Coffee break

<i>Time</i>	<i>Chairman</i>	<i>Speaker</i>		<i>Title of presentation</i>
10:30 to 12:15	Magdaléna Hromadová	<b>Roberto Spotorno</b>	IT	Rotating Fourier Transform Applied to Electrochemical Impedance Spectroscopy: New Opportunities for Low-Frequency Measurement. <i>(Introductory lecture)</i>
		<b>Fermin Sáez Pardo</b>	ES	Deep Learning Algorithm, Based on Convolutional Neural Networks, for Equivalent Electrical Circuit Recommendation for Electrochemical Impedance Spectroscopy, and its Application to an All-Iron Battery.
		<b>Chao Zhang</b>	SE	How can we bridge experiments and molecular modelling in EIS?
12:30	Lunch			
<b>Monday, June 10 – afternoon</b>				
Topic: <b>Zdravko Stoynov Memorial Medal lecture</b>				
<i>Time</i>	<i>Chairman</i>	<i>Speaker</i>		<i>Title of presentation</i>
14:00 to 16:00	Daria Vladikova	<b>Andrzej Lasia</b>	CA	Multisine and dynamic impedance spectroscopy. <i>(Plenary lecture)</i>
		<b>Gábor Mészáros</b>	HU	A noise based approach to constant phase behaviour; Is there such a thing as charge transfer resistance?
		<b>Táňa Sebechlebská</b>	SK	3D Printed Impedimetric Sensing: A New Tool for Microfluidic Analysis
		<b>Matěj Stočes</b>	CZ	Get to know Metrohm
16:00	Coffee break			
<i>Time</i>	<i>Chairman</i>	<i>Speaker</i>		<i>Title of presentation</i>
16:30 to 17:30	Dan Bizzotto	<b>Gyözö G. Láng</b>	HU	EIS analysis of PEDOT-modified electrodes – stability, thickness distribution, and non- stationarity <i>(Introductory lecture)</i>
		<b>Viliam Kolivoška</b>	CZ	Measurements of Penetrability in Antifouling Polymer Brush Nanocoatings by Electrochemical Approaches
		<b>Tomáš Kolenský</b>	CZ	Measurement of photopolymer quality during vat polymerization 3D printing by EIS
18:00	Concert (in the courtyard of the castle) <b>J-D-K-D Quartet</b>			
19:15	Dinner			
20:40	Open fire <b>sausage party</b> in the park			

<b>Tuesday, June 11 – morning</b>				
from 7:00 Breakfast				
<i>Time</i>	<i>Chairman</i>	<i>Speaker</i>		<i>Title of presentation</i>
8:30 to 10:00	Romana Sokolová	<b>Dan Bizzotto</b>	CA	Investigating heterogeneity in SAMs of redox-labelled DNA using EIS <i>(Introductory lecture)</i>
		<b>Stanislav Hasoň</b>	CZ	Differential capacitance-time measurements to study the adsorption of oligodeoxynucleotides at the basal plane-oriented pyrolytic graphite electrodes and clarify their complex voltammetric responses
		<b>Veronika Ostatná</b>	CZ	Analysis of carbohydrates on charged surfaces.
10:00 Coffee break				
<i>Time</i>	<i>Chairman</i>	<i>Speaker</i>		<i>Title of presentation</i>
10:30 to 12:00	Rafał Jurczakowski	<b>Soma Vesztegom</b>	HU	Hydrogen evolution at constant current, accompanied by time-resolved impedance monitoring.
		<b>Vitali Grozovski</b>	EE	Electrolytic hydrogen evolution on Bi metal.
		<b>Sheena Louisia</b>	NL	Disentangling the capacitive response of single crystal Pt surfaces at the onset of the alkaline hydrogen evolution reaction
12:00 Lunch				
13:15 Departure of the bus for the trip:				
14:15 <b>Gothic castle Lipnice</b>				
16:30 historic town <b>Havlíčkův Brod - Church tower and bells</b>				
17:30 <b>Traditional brewery "REBEL"</b> (Havlíčkův Brod) - excursion and degustation				
19:30 Dinner in the brewery restaurant				
22:30 Expected arrival to the castle				

<b>Wednesday, June 12 – morning</b>				
from 7:00		Breakfast		
<i>Time</i>	<i>Chairman</i>	<i>Speaker</i>		<i>Title of presentation</i>
8:30 to 10:00	Miran Gaberšček	<b>Rafał Jurczakowski</b>	PL	Equivalent circuit for assessing pore size distribution in porous electrodes by EIS. <i>(Introductory lecture)</i>
		<b>Subhasis Shit</b>	DE	Reaction kinetics in water electro-oxidation addressed by impedance spectroscopy for redox-active NiFe oxyhydroxides
		<b>Shima Farhoosh</b>	DE	Reaction Kinetics in Water Oxidation Studied by Time-resolved X-ray Absorption and Electrochemical Impedance Spectroscopy
10:00		Coffee break		
<i>Time</i>	<i>Chairman</i>	<i>Speaker</i>		<i>Title of presentation</i>
10:30 to 12:20	Gábor Mészáros	<b>Miran Gaberšček</b>	SI	Physics Based Transmission Line Models for Porous Battery Electrodes. <i>(Introductory lecture)</i>
		<b>Varsha Sasikumar</b>	IE	Electrochemical Impedance Spectroscopy Investigation of Vanadium Flow Battery Reactions at Glassy Carbon Electrodes
		<b>Blagoy Burdin</b>	BG	First Steps in Differential Resistance Analysis for battery testing
		<b>Werner Strunz</b>	DE	Validation and Reconstruction of Impedance Data – Combining Measurement Model and ZHIT Algorithm
12:30		Lunch		
<b>Wednesday, June 12 – afternoon</b>				
<i>Time</i>	<i>Chairman</i>	<i>Speaker</i>		<i>Title of presentation</i>
14:30 to 16:00	Tamás Pajkóssy	<b>Daria Vladikova</b>	BG	Accelerated Ex-situ Aging of Solid Oxide Fuel Cell Anode via Redox-cycling Investigated by Differential Impedance Analysis <i>(Introductory lecture)</i>
		<b>Milena Krapchanska</b>	BG	Artificial Aging of SOFC by Accelerated Stress Tests
		<b>Paolo Piccardo</b>	IT	EIS on all solid state Li-ion batteries with Halide based electrolyte: an insight on the battery condition during operation
16:00		Coffee break		



<i>Time</i>	<i>Chairman</i>	<i>Speaker</i>		<i>Title of presentation</i>
16:30 to 18:15	Magdaléna Hromadová	<b>Nicolas Murer</b>	FR	Non-stationary impedance: the case of the Volmer-Heyrovský corrosion reaction.
		<b>Jan Macák</b>	CZ	Electrochemical impedance spectroscopy of steels in supercritical water.
		<b>Tomáš Černoušek</b>	CZ	Electrochemical impedance spectroscopy measurement of microbially influenced corrosion.
		<b>Lubomír Pospíšil</b>	CZ	Electrochemical Impedance of Organic Multiple Redox Sites.
18:30	Walk around Třešť			
20:00	<b>Farewell dinner</b>			

### Thursday, June 13 – morning

from

7:00 Breakfast

8:30 – 9:00 Please, leave the rooms – check out – put luggage in checkroom

Topic: <b>Tutorial Session</b>				
<i>Time</i>	<i>Chairman</i>	<i>Speaker</i>		<i>Title of presentation</i>
9:00 to 10:15	Daria Vladikova	<b>Tamás Pajkóssy</b>	HU	1. Basics of electrochemical impedance spectroscopy EIS 2. Experimental aspects of EIS
10:15	Coffee break			
Topic: <b>Q &amp; A Session with Companies</b>				
<i>Time</i>	<i>Chairman</i>	<i>Representative</i>		<i>Company Name</i>
10:45 to 11:45	Magdaléna Hromadová	<b>Werner Strunz, Alexander Krimalowski</b>		<i>Zahner-Elektrik GmbH &amp; Co KG</i>
		<b>Nicolas Murer</b>		<i>BioLogic SAS</i>
				General Discussion on EIA
11:45	Closing remarks			
12:00	Lunch			
13:30	Departure to Prague			
16:30	expected arrival at the <b>Václav Havel Airport Prague</b>			

**32 oral presentations and 5 posters  
(42 attendees)**

**POSTERS** SHOULD BE ON DURING THE WHOLE MEETING  
IN THE FOYER OF THE CONFERENCE HALL  
(No special poster session will be organized, discussion may proceed  
during coffee-breaks and after sessions)

**POSTERS**

<b>Lucie Dostálková</b> CZ	Electrochemical Behaviour of Selaginpulvilins.
<b>Vitali Grozovski</b> EE	Ion-selective Desalination Materials.
<b>Jakub Jambrich</b> DE	Investigation of LTO Anodes as a Reference for EIS and NFRA Measurements.
<b>Kamil Jaššo</b> CZ	Electrochemical Impedance Spectroscopy for Lithium-Ion Batteries.
<b>Alice Kulagová</b> CZ	Electrochemical Characterization of Polymerized Supramolecular Grids on Electrode Surfaces.

# ORAL PRESENTATIONS

(ALPHABETICAL LIST)

# Investigating Heterogeneity in SAMs of Redox-labelled DNA Using EIS

Dan Bizzotto, Tianxiao Ma, Diana Baker, and Gilberto Martinez

<sup>a</sup> AMPEL & Department of Chemistry, University of British Columbia, 2036 Main Mall, Vancouver, BC, Canada, bizzotto@chem.ubc.ca

Alkylthiol modified DNA was used to prepare self-assembled monolayers on a gold single crystal bead electrode. The DNA was further modified on the distal end with a methylene blue redox-active label. This type of modified electrode is often used for DNA sensing<sup>1-3</sup>, but a number of interesting questions remain regarding the nature of the modified surface and the influence of the local interfacial environment on the kinetics of the redox label. EIS was used to characterize these interfaces using one or two time constants, following Creager.<sup>4,5</sup> The amount of MB measured and the redox rate was determined and compared to CV and SWV measurements of single-stranded DNA (ssDNA) SAMs. Hybridization with the complementary target strand from solution was found to decrease the average redox kinetics. This can be understood as the presence of MB-labelled DNA in two categories: either fast redox (ssDNA) or slow redox (double stranded DNA (dsDNA) SAM). Analysis of the EIS data collected for these interfaces were done using equivalent circuits with one or two series RC time constants.<sup>4,6,7</sup>

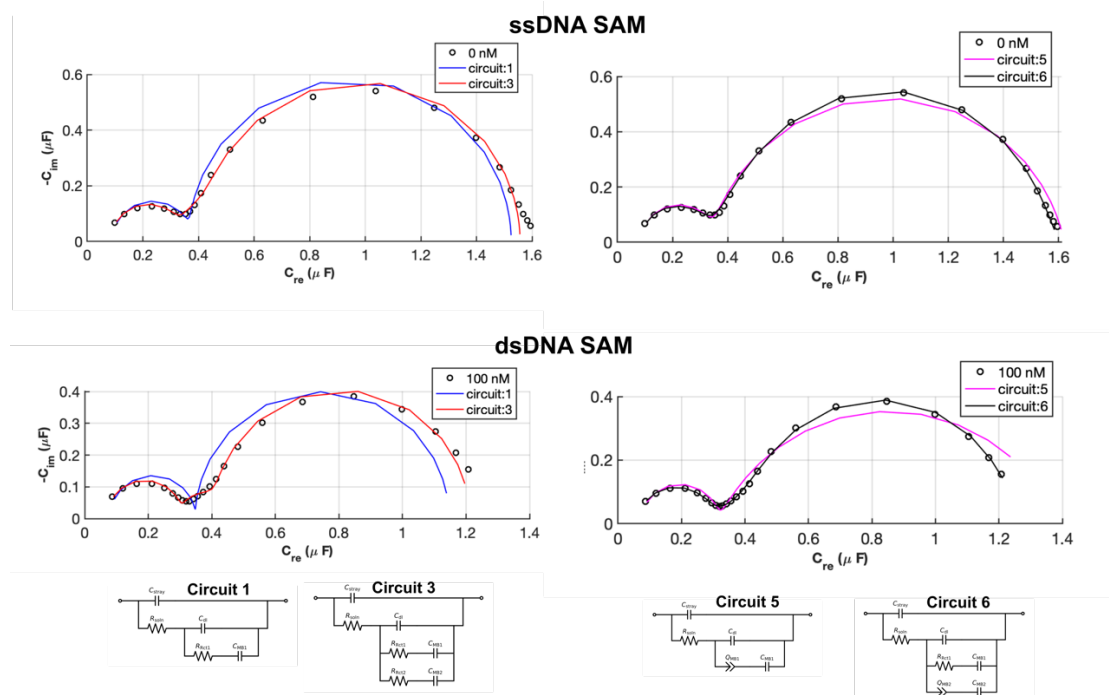


**Fig. 1:** Complex capacitance representations of redox-labelled DNA SAMs and fits of the data to four equivalent circuits. Top row is single-stranded DNA SAM and the bottom row is after equilibration with 100 nM of the complementary target.

Figure 1 shows the complex capacitance representation of the EIS data and the fitting for ssDNA and dsDNA SAMs to four different equivalent circuits. One or two RC time constants were able to fit the ssDNA SAM. Two time constants were required to fit the dsDNA SAM suggesting the presence of unhybridized ssDNA remaining in the SAM. The average rate of electron transfer decreased from  $37\text{s}^{-1}$  for ssDNA SAM to  $5\text{s}^{-1}$  for the dsDNA SAM, as expected<sup>2,7,8</sup>. This change was coupled with a decrease in the amount of redox active MB (loss of 20%). A further modification of the equivalent circuit to introduce a Cole-Cole like time constant distribution<sup>6,9</sup>

showed the presence of two rates for the dsDNA SAM: 60% had  $5\text{s}^{-1}$  and 40 % had a distributed rate constant with a maximum of  $2\text{s}^{-1}$ . Other DNA SAMs prepared using a different procedure (e.g., higher coverage, pre-hybridized before SAM formation, location of the redox-active MB label) were analyzed and the results will be discussed in terms of non-uniformity of the DNA SAMs.

### References

1. E. E. Ferapontova, *Annual Review of Analytical Chemistry*, **11**, 197–218 (2018).
2. P. Dauphin-Ducharme and K. W. Plaxco, *Anal. Chem.*, **88**, 11654–11662 (2016).
3. R. White and K. W. Plaxco, *Anal. Chem.*, **82**, 73–76 (2009).
4. J. Li, K. Schuler, and S. E. Creager, *Journal of The Electrochemical Society*, **147**, 4584 (2000).
5. S. E. Creager and T. T. Wooster, *Analytical Chemistry*, **70**, 4257–4263 (1998).
6. Lasia, Andrzej, *Electrochemical Impedance Spectroscopy and its Applications*, Springer New York, New York, NY, (2014).
7. T. Uzawa, R. R. Cheng, R. J. White, D. E. Makarov, and K. W. Plaxco, *J. Am. Chem. Soc.*, **132**, 16120–16126 (2010).
8. P. Dauphin-Ducharme, N. Arroyo-Curras, and K. W. Plaxco, *Journal of the American Chemical Society*, **141**, 1304–1311 (2019).
9. Dr. E. Barsoukov and Dr. J. R. Macdonald, *Impedance spectroscopy*, (2022)  
<https://doi.org/10.1002/9781119381860>.

## First Steps in Differential Resistance Analysis for Battery Testing

Blagoy Burdin<sup>a,b</sup>, Daria Vladikova<sup>a,b</sup> and Dimitar Bojchev<sup>a</sup>

<sup>a</sup> *Institute of Electrochemistry and Energy Systems – Bulgarian Academy of Sciences, 10 Acad. G. Bonchev, 1113 Sofia, Bulgaria, b.burdin@iees.bas.bg;*

<sup>b</sup> *Institute for Sustainable Transition and Development – Trakia University, Students Campus, 6000 Stara Zagora, Bulgaria*

The battery State of Health (SoH) is a parameter that should present the general state of the battery at a given moment of its operation. There are a number of methods and criteria for determining SoH, but they do not give clear assessment for the battery state and its moment ability to meet the given requirements.

In the present work we show first results concerning a new approach for battery SoH determination. The method is based on the Differential Resistance Analysis (DRA) which we apply on battery i-V curves. Firstly it was developed and tested on solid oxide fuel cells for degradation monitoring and evaluation of the degradation rate. The main advantages of the new approach are the increased sensitivity and information capability due to the application of derivatives [1,2].

For the introduction of DRA in batteries, the presence of one more variable should be overcome – the parameter State of Charge (SOC) which does not exist in fuel cells. Since the capacity of the battery changes (decreases) during its life, a working algorithm has been developed to determine the SoH at a defined capacity. For this purpose, the concept of instantaneous capacity  $C_m$  was introduced, which represents the capacity of the battery at a certain moment, after carrying out a definite number of charge/discharge cycles. The testing procedure includes:

- aging through charge/discharge cycles;
- measurement of the battery capacity at a certain moment of aging;
- full charge of the battery followed by i-V curve measurements which are carried out in selected states of charge in respect to the instantaneous capacity. Initially, the measurements are carried out in the first defined state - 100% SOC;
- impedance measurements at selected operating points of the i-V curve. The first selected points are at 3% and 30% of the maximum allowable current for the respective battery condition. The third operating point is the minimum value of the differential resistance –  $R_{d,min}$ ;
- the procedure is repeated from the initial state of the battery to the end of life through a certain number of charge/discharge cycles.

For determination of the SoH, a characteristic point of the i-V curve is selected. The point corresponds to the minimum value of  $R_{d,min}$  and depends only on the condition of the battery, but not on the given operating parameters. Therefore,  $R_{d,min}$  should appear in different places in the i-V curves depending on the load.

The experiments were carried out on a “LAVA” Li-ion Battery 18650 with a capacity of 2200mAh and nominal voltage 3,7V. To reduce the testing time, the approach of accelerated battery aging by increasing the magnitude of the discharge current was applied. The discharge current (C-rate) at which aging is accelerated without reaching a state of irreversible battery damage has been experimentally determined. It was found that the optimal value of the discharge current for the tested batteries is in the range of 1C – 1,5C.

Fig.1 shows displacement of  $R_{d,min}$  position during aging and the corresponding impedance diagrams measured at the  $R_{d,min}$  working points.

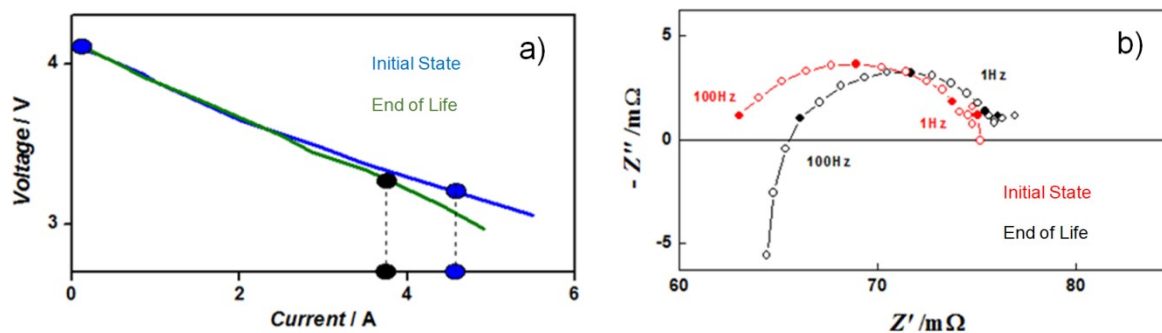


Fig.1: a)  $i$ - $V$  curves and b) impedance diagrams in Initial state and End of life measured at 100% SoC.

### Acknowledgements

The authors acknowledge the support of the Bulgarian Ministry of Education and Science under the: (i) National Roadmap for Research Infrastructure 2017-2023 "Energy storage and hydrogen energetics (ESHER)", approved by DCM № 354/29.08.2017, (ii) Bulgarian National Recovery and Resilience Plan, Component "Innovative Bulgaria", Project № BG-RRP-2.004-0006-C02 "Development of research and innovation at Trakia University in service of health and sustainable well-being" and (iii) National Research Programme E+: Low Carbon Energy for the Transport and Households, grant agreement D01-214/2018.

### References

- [1] Stoynov, Z., Vladikova, D., Burdin, B. Differential Resistance Analysis – Current Achievements and Applications. *Bulgarian Chemical Communications*, Volume 50, Special Issue D, 2018, 21-30., 50, Special Issue D, 2018, 21-30.
- [2] Stoynov, Z., Vladikova, D., Burdin, B., Laurencin, J., Montinaro, D., Raikova, G., Schiller, G., Szabo, P. Differential analysis of SOFC current-voltage characteristics. *Applied Energy*, 288, Elsevier Ltd., 2018, ISSN: 0306-2619, DOI:doi.org/10.1016/j.apenergy.2018.06.138, 1584-1590

## Electrochemical Impedance Spectroscopy Measurement of Microbially Influenced Corrosion

Tomáš Černoušek<sup>a</sup>,

<sup>a</sup> Department of Material Analysis, Research Centre Řež Ltd., Hlavní 130, 250 68 Husinec-Řež, Czech Republic, [tomas.cernousek@cvrez.cz](mailto:tomas.cernousek@cvrez.cz)

Microbially influenced corrosion (MIC) is a form of corrosion that may limit the lifetime of nuclear waste canisters in long term. Electrochemical impedance spectroscopy (EIS) represent an excellent method for investigation the impact of microorganisms on corrosion behavior in long-term monitoring studies. EIS measurements from a long-term study on carbon steel corrosion in deep natural groundwater containing sulfate-reducing bacteria illustrate the impact microbial activity on the corrosion processes in the impedance data. Measurement of EIS shows the evolution of three time constant under abiotic conditions, in connection with the formation of two layers of biofilms. Molecular-biological analysis of the water and biofilm indicated the dominance of SRB, with *Desulfomicrobium* and *Desulfovibrio* species prevalent [1, 2].

### References

- [1] Černoušek, T., Shrestha, R., Kovářová, H., Špánek, R., Ševců, A., Sihelská, K., Steinová, J. (2020). Microbially influenced corrosion of carbon steel in the presence of anaerobic sulphate-reducing bacteria. *Corrosion Engineering, Science and Technology*, 55(2), 127–137. <https://doi.org/10.1080/1478422X.2019.1700642>
- [2] Tomáš Černoušek, Alena Ševců, Rojina Shrestha, Jana Steinová, Jakub Kokinda, Kateřina Vizelková, Chapter 6 - Microbially influenced corrosion of container material, Editor(s): Jonathan R. Lloyd, Andrea Cherkouk, *The Microbiology of Nuclear Waste Disposal*, Elsevier, 2021, Pages 119-136, ISBN 9780128186954, <https://doi.org/10.1016/B978-0-12-818695-4.00006-X>.



## Reaction Kinetics in Water Oxidation Studied by Time-Resolved X-Ray Absorption and Electrochemical Impedance Spectroscopy

Shima Farhoosh<sup>a</sup>, Holger Dau<sup>a</sup>

<sup>a</sup> *Department of Physics, Freie Universität Berlin, Arnimallee 14, 14195, Berlin, Germany, shima.farhoosh@fu-berlin.de*

Water splitting driven by ‘green electricity’ is a promising approach for the production of hydrogen, which can serve as a synthetic fuel or be used to generate further valuable chemicals. A cobalt-based oxy-hydroxide electrocatalyst (CoCat) favourably supports the oxygen evolution reaction (OER) at neutral pH.<sup>[1-2]</sup> The cobalt ions of the bulk-active material undergo redox reactions that precede the O-O bond formation chemistry.<sup>[3]</sup> We investigated the kinetics of redox transitions and electrocatalysis by combining analyses of time-resolved X-ray absorption spectroscopy (XAS) and electrochemical impedance spectroscopy (EIS). Discrimination between the influence of chemical reaction kinetics and charge transport limitations was achieved by comparative analysis of catalyst films with thicknesses ranging from 35 nm to 560 nm, inter alia revealing that the redox transitions of interacting cobalt sites occur rapidly, within milliseconds, while the OER proceeds significantly slower.

### References

- [1] S. Liu, I. Zaharieva, L. D’Amario, S. Mebs, P. Kubella, F. Yang, P. Beyer, M. Haumann, H. Dau, *Adv. Energy Mater.* 2022, 12, 2202914.
- [2] S. Liu, S. Farhoosh, P. Beyer, S. Mebs, I. Zaharieva, M. Haumann, H. Dau, *Adv. Sustainable Syst.* 2023, 7, 2300008.
- [3] M. Risch, F. Ringleb, M. Kohlhoff, P. Bogdanoff, P. Chernev, I. Zaharieva, H. Dau *Energy Env. Science* 8, 661-67

## Physics Based Transmission Line Models for Porous Battery Electrodes

Miran Gaberšček<sup>a,b</sup>

<sup>a</sup>*National Institute of Chemistry, Hajdrihova 19, 1000 Ljubljana, Slovenia*

<sup>b</sup>*Faculty of Chemistry and Chem. Technol. University of Ljubljana, 1000 Ljubljana, Slovenia*  
*miran.gaberscek@ki.si*

Modern battery electrodes are intricate systems comprised of a vast number of active particles, often reaching up to  $10^{14}$  per square centimeter of metallic substrate. Additionally, they encompass at least three to four other phases, including binders, coatings, conductive additives, and electrolytes, all crucial for their proper functionality. Optimising the mass and charge transport within such complex configurations presents inherent challenges. This complexity contrasts sharply with the relatively limited features observed in impedance spectra of battery electrodes, typically manifesting as one or two arcs and a diffusion-related line. Consequently, analyzing battery processes using impedance spectroscopy, or any electrochemical technique, proves challenging, if not ambiguous.

To address this inherent difficulty, we have recently proposed various experimental approaches that help collect essential battery parameters in a systematic way. Once such data have been collected, a suitable model is needed for the consistent interpretation of measured impedance responses. Recent investigations have revealed that physics-based transmission line modeling presents a compelling compromise between accuracy, speed and flexibility of data analysis. More specifically, this modeling approach yields accurate information regarding pertinent physical parameters—such as diffusion coefficients, transport numbers, conductivities, exchange current density, and contact resistances—while remaining computationally efficient, typically requiring only 5 to 10 seconds per spectrum.

We intend to illustrate the aforementioned experiment-based modeling approach using several battery electrodes and cells of practical significance, showcasing its efficacy in understanding and optimizing battery performance.

## Electrolytic Hydrogen Evolution on Bi Metal

Vitali Grozovski<sup>a</sup>, Syed Muhammad Kumail Mehdi Abidi<sup>a</sup>, Soma Vesztergom<sup>b</sup>, Jaak Nerut<sup>a</sup>, Enn Lust<sup>a</sup>

<sup>a</sup>*Institute of Chemistry, University of Tartu, Ravila 14a, Tartu, 50411 Estonia*

<sup>b</sup>*Department of Physical Chemistry, Eötvös Loránd University, 1117 Budapest, Hungary*  
vitali.grozovski@ut.ee

Cathodic hydrogen evolution is one of the most extensively researched electrode processes in electrochemistry. However, in the profile literature, we still need help finding direct answers to some very straightforward problems, such as how much the change in surface pH during hydrogen evolution affects the system's content. Previous research has aimed to address this topic for rotating disk electrodes [1,2]. It is time to extend this model to characterize constant current hydrogen evolution studies on stationary electrodes with high hydrogen overvoltage. This work involved galvanostatic electrolysis on a bismuth single crystal Bi(111) working electrode. According to the previous cyclic voltammetry, impedance, chrono-coulometry, and STM studies [3-5], there is no quick surface reconstruction of Bi(hkl) within the region of ideal polarizability. The electrolyte was a moderately acidic (pH = 2.5, acidified with perchloric acid) sodium perchlorate solution. The chronopotentiograms obtained with different cathodic current densities during the electrolysis show good agreement with the model proposed in this study. The model's aspect is that hydrogen evolution is described by a single charge transfer reaction unaffected by medium pH. The transport of H<sup>+</sup> and OH<sup>-</sup> ions is handled as if the two diffusion coefficients are equal, while the equilibrium constraint governed by water autoprotolysis is also appraised.

### References

- [1] V. Grozovski, S. Vesztergom, G.G. Láng, P. Broekmann, *J. Electrochem. Soc.* 164 (11) (2017) E3171-E3178.
- [2] M. J. Gálvez-Vázquez, V. Grozovski, N. Kovács, P. Broekmann, S. Vesztergom, *J. Phys. Chem. C* 124(7) (2020) 3988-4000
- [3] S. Trasatti, E. Lust, The Potential of Zero Charge, in: White, R.E., Bockris, J.O'M., Conway, B.E. (Eds.), *Mod. Asp. Electrochem.*, Kluwer Academic / Plenum Publishers, New York, 1999: pp. 1–193.
- [4] S. Kallip, E. Lust, *Electrochem. Commun.* 7 (2005) 863–867.
- [5] R. Jäger, S. Kallip, V. Grozovski, K. Lust, E. Lust, *J. Electroanal. Chem.* 622 (2008) 79–89.

## Differential Capacitance-Time Measurements to Study the Adsorption of Oligodeoxynucleotides at the Basal Plane-Oriented Pyrolytic Graphite Electrodes and Clarify their Complex Voltammetric Responses

Stanislav Hasoň, Veronika Ostatná, Miroslav Fojta

*Institute of Biophysics, The Czech Academy of Sciences, Kralovopolska 2590/135, CZ-61200, Brno, Czech Republic, e-mail: hasons@ibp.cz*

We show that measuring the time dependence of the differential capacitance ( $C_d - t$  curves) of basal plane-oriented pyrolytic graphite (BPGE) before and after the addition of individual oligodeoxynucleotide molecules (ODNs) can help clarify their complex voltammetric responses. As shown earlier, the resulting current densities of ODN electro-oxidation peaks are the sum of the current contributions of both diffusing ODNs to the electrode surface and those adsorbing on it [1]. Therefore, a more detailed description of the adsorption behavior of ODNs on the electrode surface using  $C_d - t$  curves can reveal the influence of ODN structure on the organization of the electric double layer at the charged interface.

An example is the complex voltammetric response of purine residues of an acid-hydrolyzed ODN duplex ( $d(\text{GA})_5 + d(\text{TC})_7$ ) containing both purine and pyrimidine residues. The acid-hydrolyzed  $d(\text{GA})_5$  ( $ah-(\text{GA})_5$ ) produced the voltammogram, which is characterized by two single electro-oxidation peaks at potentials of +0.73 V (peak  $\text{G}^{\text{ox}}$ ) and +1.0 V (peak  $\text{A}^{\text{ox}}$ ) (Figure 1Ba). These peaks are associated with the electro-oxidation of free guanine (G) and adenine (A) nucleobases, respectively (Figure 1A). This is consistent with biochemical experiments showing a 100% release of purine nucleobases from DNA during acid hydrolysis [2]. We experimentally confirmed this conclusion by the  $C_d - t$  curves, where the  $C_d - t$  curve of  $ah-(\text{GA})_5$  had an almost identical, slowly decreasing exponential decay (dashed pink in Figure 1C) as the  $C_d - t$  curve describing the adsorption of the same number of free G and A nucleobases from their equimolar mixture on BPGE surface (pink dots in Figure 1C). In general, the drop of  $C_d$  of BPGE after the addition of molecules (ODNs and/or free nucleobases) below the  $C_d$  characterizing BPGE surface in the background electrolyte (gray curve in Figures 1C and 1D) is a result of displacement of water molecules with a higher dielectric constant by ODN and/or free nucleobases with lower relative permittivity values [3, 4]. Conversely, the  $C_d - t$  curve of the adsorbing  $d(\text{GA})_5$  has an initial steep exponential decline (purple open circles in Figure 1C), indicating rapid and strong adsorption.

The acid-hydrolyzed ODN duplex gave about 67% lower  $\text{G}^{\text{ox}}$  and  $\text{A}^{\text{ox}}$  peaks than the same numbers of released G and A nucleobases in  $ah-(\text{GA})_5$ . In addition, two new peaks  $\text{G}'^{\text{ox}}$  and  $\text{A}'^{\text{ox}}$  appeared in the voltammogram at potentials of +0.83 and +1.2 V, respectively (Figure 1Bb).

The measurement of the  $C_d - t$  curves of both intact ( $d(\text{TC})_7$ ) and acid-hydrolyzed ( $ah-(\text{TC})_7$ ) ODN  $d(\text{TC})_7$  helped to explain the origin of the  $\text{G}'^{\text{ox}}$  and  $\text{A}'^{\text{ox}}$  peaks. The sharp, almost identical exponential decay in the  $C_d$  values for both  $d(\text{TC})_7$  (open black circles in Figure 1D) and  $ah-(\text{TC})_7$  (dashed light brown in Figure 1D) assumes very rapid and strong adsorption of the  $ah-(\text{TC})_7$  on the BPGE surface. On the contrary, free cytosine and thymine nucleobases adsorption in the number corresponding to the  $ah-(\text{TC})_7$  has a considerably slower exponential decay during 10-min adsorption without reaching saturation (light brown dots in Figure 1D). This confirms the earlier assumption of only a negligible release of pyrimidine nucleobases from the acid-hydrolyzed DNA molecule during 30-min treated interval [2].

We can assume that during the competitive adsorption of d(TC)<sub>7</sub> together with free G and A nucleobases, only part of the purine nucleobases came into direct contact with the BPGE surface (resulting in a dramatic drop in the heights of the G<sup>ox</sup> and A<sup>ox</sup> peaks in Figure 1Bb). Another part of free purine nucleobases had to overcome the adsorbed d(TC)<sub>7</sub> layer before interacting with the electrode surface. At a higher positive electrode polarization, the free purine nucleobases will gain enough energy to be electro-oxidized through the adsorbed layer of the d(TC)<sub>7</sub> and produce their electro-oxidation peaks at more positive potentials.

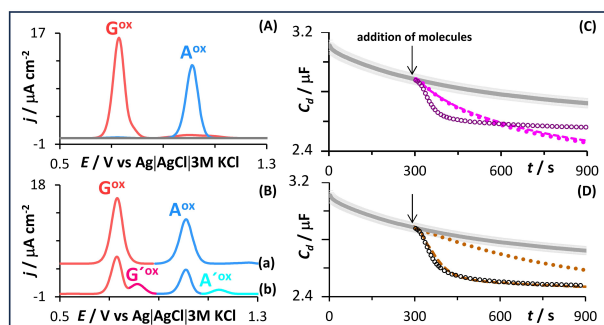


**Fig 1:** (A, B) Baseline-corrected adsorptive stripping differential pulse voltammograms of (A) 1  $\mu\text{M}$  G (red) and 1  $\mu\text{M}$  A (blue), (Ba) 300 nM acid-hydrolyzed d(GA)<sub>5</sub>, and (Bb) 300 nM acid-hydrolyzed ODN duplex formed by d(GA)<sub>5</sub> + d(TC)<sub>7</sub> measured on a basal plane-oriented pyrolytic graphite electrode (BPGE). (C, D) Differential capacitance – time curves ( $C_d - t$  curves) of BPGE measured in 0.1 M acetate buffer before and after addition (black arrows) of (C) 900 nM d(GA)<sub>5</sub> (purple open circles), 900 nM acid-hydrolyzed d(GA)<sub>5</sub> (dashed pink), and 4.5  $\mu\text{M}$  equimolar mixture of G and A (pink dots), (D) 643 nM d(TC)<sub>7</sub> (black open circles), 643 nM acid-hydrolyzed d(TC)<sub>7</sub> (dashed light brown), and 4.5  $\mu\text{M}$  equimolar mixture of cytosine and thymine (light brown dots). The gray curves represent the measurement in the background electrolyte (0.1 M acetate buffer).

### Acknowledgement

This work was supported by The Czech Academy of Sciences (No. 68081707).

### References

- [1] L.M. Goncalves, C. Batchelor-Mcauley, A.A. Barros, R.G. Compton, *J. Phys. Chem. C* 114 (2010) 1413.
- [2] R. Shapiro, M. Danzig, *Biochem. Biophys. Acta* 319 (1973) 5.
- [3] P. Capaldo, S.R. Alfano, L. Ianeselli, S.D. Zilio, A. Bosco, P. Parisse, L. Casalis, *ACS Sensors* 1 (2016) 1003.
- [4] S. Hason, V. Ostatna, M. Fojta, *Electrochim Acta* 441 (2023) 141772.

## Equivalent Circuit for Assessing Pore Size Distribution in Porous Electrodes by EIS

Anna Plis, Piotr Połczyński, Rafał Jurczakowski

University of Warsaw, Faculty of Chemistry, Laboratory of Electroanalytical Chemistry, Pasteur 1, PL-02-089, Poland, rafjur@chem.uw.edu.pl

Porous electrodes play a crucial role in applications of electrochemical systems. Smooth electrodes are not practical as they would require very large surface area to achieve similar efficiency. In industrial electrolysis, energy conversion and storage, porous electrodes are therefore frequently employed.

Electrochemical impedance spectroscopy (EIS) is a powerful, non-invasive diagnostic tool that can be used to characterize porous conductive media. It is well known that pore geometry can greatly impact the performance of supercapacitors and the activity of electrocatalysts. Porous materials, such as activated carbons and carbon fibers, frequently show a log-normal distribution in pore size. However, to date, the impedance of porous electrodes characterized by such distribution has been described only in terms of numerical models [1, 2].

In this report, we provide analytical solutions for impedance of porous electrodes having unequal pores radii described by log-normal distribution. The model is valid in the low and high frequency range [3].

Provided equivalent circuit and analytical expressions enable a comprehensive characterization of porosity of conductive materials. We demonstrate that key parameters of electrode porosity can be easily found even from a single impedance spectrum. Moreover, the width of the pore size distribution can be determined solely from impedance data, without requiring any additional information on the system being studied [3]. Additionally, the mean pore radius, pore depth, and number of pores can be also determined if the total pore volume,  $V_{\text{tot}}$ , and double layer capacity,  $C_{\text{dl}}$ , are known. It should be noted that both  $V_{\text{tot}}$  and  $C_{\text{dl}}$  parameters are relatively easily accessible experimentally.

The model also considers the non-ideal CPE behaviour of porous electrodes often seen in real systems. We applied this model to analyse the electrochemical impedance of activated carbon electrodes in a sulphuric acid solution, showing that key porosity parameters can be determined even from a single impedance spectrum [3].

Considering the influence of double layer formation on the effective micropore sizes, the use of classical porosimetry for electrochemical applications could lead to significant inaccuracies. In contrast, the developed model allows for more realistic determination of effective pore sizes in electrochemical systems. Hence, the model can be used to establish possible geometric factors limiting the activity of catalysts or the efficiency of energy storage devices.

### References:

- [1] H.K. Song, Y.H. Jung, K.H. Lee, L.H. Dao, *Electrochim. Acta* 44 (1999) 3513
- [2] M Musiani, M Orazem, B Tribollet, V. Vivier, *Electrochim. Acta* 56 (2011) 8014.
- [3] A. Plis, P. Połczyński, R. Jurczakowski, *Electrochem. Commun.* 164 (2024) 107716

# Measurement of Photopolymer Quality during Vat Polymerization 3D Printing by EIS

Tomáš Kolenský<sup>a</sup>, Kamil Jaššo<sup>a</sup>

<sup>a</sup> Faculty of Military Technology, University of Defence in Brno, Kounicova 65, 662 10, Brno, Czech republic, tomas.kolensky@unob.cz, kamil.jasso@unob.cz

Over the past few years, additive manufacturing (AM) has gained an increasingly important role in the production of not only prototypes but also in the field of manufacturing functional parts in larger quantities. This paper focuses on photopolymers used in the vat polymerization 3D printing technique, which is one of several AM techniques [1]. When discussing vat polymerization, we must first consider the technique of processing the base material, in this case, the photopolymer, and then the photopolymer itself. Photopolymers are primarily composed of oligomers, monomers, and photoinitiators. The quantity and type of materials used can drastically alter the properties of the photopolymer and, therefore, the properties of the printed object. Additionally, the base material exhibits aging, which adversely affects its properties and can eventually lead to defective prints [2]. We can utilize electrochemical impedance spectroscopy (EIS) to measure the electrochemical properties of the base material and use it to create standard models of photopolymer quality. This model can be easily compared with measured samples of photopolymers inside the printing vat before and during printing. Due to the non-destructive nature of the EIS method, measurements can be performed directly on the material used during 3D printing without any effects on the printed object. We measured three samples of the same photopolymer in different states: firstly, we measured new photopolymer from the bottle, then we left two samples for one week in the printer, one with a covered vat and one with an opened vat, and then we measured them. From the measurements, it is clear that due to the evaporation of the photoinitiator used in the resin, the photopolymer degrades and printing could tend to fail. There is also a greater risk of insufficient polymerization and risk of delamination of the material. Our aim is to create an in-vat electrode capable of direct measurements before and during printing [3]. This is also important because the recommended printing temperature for vat polymerization is 25°C, which leads to faster evaporation of the photoinitiator and further degradation of the photopolymer.

## Acknowledgements

This work has been supported by GA ČR under grant no. 24-12982S, and Student Grant Competition of the University of Defence under the project No. 24/217-2. For research, the infrastructure of K217 Department, UD Brno, was used.

## References

- [1] L.J. Kumar, P.M. Pandey, D.I. Wimpenny, (Eds.) 3D Printing and Additive Manufacturing Technologies, 1st ed.; Springer: Berlin, Germany, 2019; ISBN 978-981-13-0305-0.
- [2] S. C. Ligon, R. Liska, J. Stampfl, M. Gurr and R. Mülhaupt, Polymers for 3d printing and customized additive manufacturing, Chem. Rev. 117 (15) (2017) 10212–10290, <https://doi.org/10.1021/acs.chemrev.7b00074>. Issn 0009-2665.
- [3] J. Minář, J. Půlpán, P. Veselý, O. Šefl and K. Dušek, "Electrical Properties of Photopolymers for 3D Printing," 2021 44th International Spring Seminar on Electronics Technology (ISSE), Bautzen, Germany, 2021, pp. 1-5, doi: 10.1109/ISSE51996.2021.9467515.

## Measurements of Penetrability in Antifouling Polymer Brush Nanocoatings by Electrochemical Approaches

Judita Anthi<sup>a,b</sup>, Eva Vaněčková<sup>c</sup>, Monika Spasovová<sup>a</sup>, Milan Houska<sup>a</sup>, Markéta Vrabcová<sup>a</sup>, Eva Vogelová<sup>a</sup>, Barbora Holubová<sup>b</sup>, Hana Vaisocherová-Lísalová<sup>a</sup>, Viliam Kolivoška<sup>c</sup>

<sup>a</sup> Department of Optical and Biophysical Systems, FZU - Institute of Physics of the Czech Academy of Sciences, Na Slovance 2, 182 00, Prague, Czech Republic

<sup>b</sup> Department of Biochemistry and Microbiology, University of Chemistry and Technology Prague, Technická 3, 166 28, Prague, Czech Republic

<sup>c</sup> Department of Electrochemistry at the Nanoscale, J. Heyrovský Institute of Physical Chemistry of the Czech Academy of Sciences, Dolejškova 3, 182 23, Prague, Czech Republic, [viliam.kolivoska@jh-inst.cas.cz](mailto:viliam.kolivoska@jh-inst.cas.cz)

Ultrathin surface-tethered polymer brushes (Fig. 1) represent attractive platforms for a wide range of sensing applications in strategically vital areas such as medicine, forensics, or security. The recent trends in such developments towards “real world conditions” highlighted the role of zwitterionic poly(carboxybetaine) (pCB) brushes which provide excellent antifouling properties combined with bio-functionalization capacity. Highly dense pCB brushes are usually prepared by the “grafting from” polymerization triggered by initiators on self-assembled monolayers (SAMs). In this contribution, multi-methodological experimental studies are pursued to elucidate the impact of the alkanethiolate SAM chain length (C<sub>6</sub>, C<sub>8</sub> and C<sub>11</sub>) on structural and functional properties of antifouling poly(carboxybetaine methacrylamide) (pCBMAA) brush. Cyclic voltammetry (CV) and electrochemical impedance spectroscopy (EIS) in a custom-made 3D printed cell employing [Ru(NH<sub>3</sub>)<sub>6</sub>]<sup>3+/2+</sup> redox probe are used to investigate penetrability of SAM/pCBMAA bilayers for small molecules and interfacial charge transfer characteristics (Fig. 1 right). The biofouling resistance of pCBMAA brushes is characterized by surface plasmon resonance (Fig. 1 left); ellipsometry and FT-IRRAS spectroscopy are used to determine swelling and relative density of the brushes synthesized from initiator-bearing SAMs with varied carbon chain length. The SAM length is found to have a substantial impact on all studied characteristics; the highest value of charge transfer resistance ( $R_{ct}$ ) is observed for denser pCBMAA on longer-chain (C<sub>11</sub>) SAM when compared to shorter (C<sub>8</sub>/C<sub>6</sub>) SAMs (Fig. 2). The observed high value of  $R_{ct}$  for C<sub>11</sub> implies a limitation for the analytical performance of electrochemical sensing methods. At the same time, the pCBMAA brushes on C<sub>11</sub> SAM exhibits the best bio-fouling resistance among inspected systems. This demonstrates that proper selection of supporting structures for brushes is critical in the design of these assemblies for biosensing applications. [1]



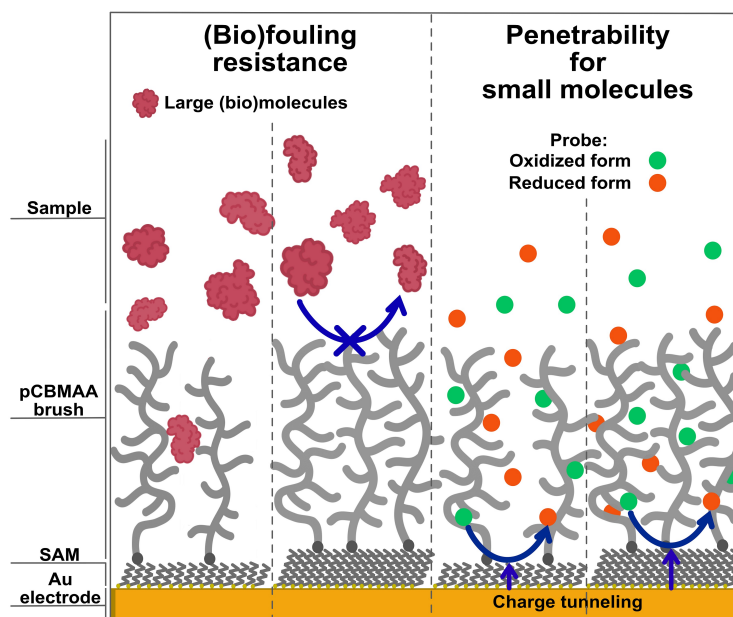


**Fig. 1:** Schematic depiction of (left) anti-fouling resistance measured by surface plasmon resonance and (right) penetrability for redox-active probe of pCBMAA brush grown on C<sub>6</sub> and C<sub>11</sub> SAMs by EIS.

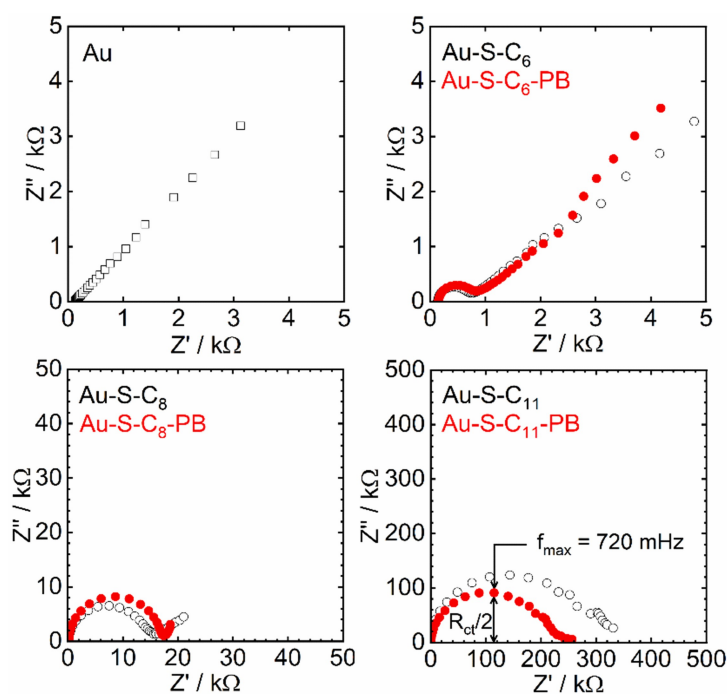


**Fig. 2:** Representative EIS response of (A) bare gold (empty squares) and gold modified by (B) C<sub>6</sub>, (C) C<sub>8</sub> and (D) C<sub>11</sub> SAM, either without (empty black circles) or with (full red circles) pCBMAA brush, obtained in de-aerated 1 mM solution of [Ru(NH<sub>3</sub>)<sub>6</sub>]Cl<sub>3</sub> probe in phosphate buffer saline supporting electrolyte at  $E^0$  of the probe in the frequency range of 10<sup>5</sup> to 10<sup>-3</sup> Hz.

## References

- [1] J. Anthi, E. Vaněčková, M. Spasovová, M. Houska, M. Vrabcová, E. Vogelová, B. Holubová, H. Vaisocherová-Lísalová, V. Kolivoška. *Anal. Chim. Acta*, 1276 (2023) 341640.

## Artificial Aging of SOFC by Accelerated Stress Tests

Milena Krapchanska<sup>a,b</sup>, Blagoy Burdin<sup>a,b</sup>, Asrar Sheikh<sup>b</sup>, Daria Vladikova<sup>a,b</sup>

<sup>a</sup> *Institute of Electrochemistry and Energy Systems, Bulgarian Academy of Sciences, 10 Acad. G. Bonchev, 1113 Sofia, Bulgaria; m.krapchanska@iees.bas.bg (M.K.), b.burdin@iees.bas.bg (B.B.), asrarskh@gmail.com (A.S.), d.vladikova@iees.bas.bg (D.V.)*

<sup>b</sup> *Institute for Sustainable Transition and Development, Trakia University, Students Campus, 6000 Stara Zagora, Bulgaria*

Fuel cells were invented over a century ago. They are unique in that they can be used for a wide range of applications, from generating power for satellites and space capsules, to powering fuel cell vehicles (automobiles, buses, trains and boats), to generating primary or emergency backup power for buildings. For decades, experts have considered solid oxide fuel cells (SOFCs) to hold the greatest potential of any fuel cell technology due to their extremely high electrical efficiencies and low operating costs. In fact, SOFCs are likely to emerge as the fastest growing fuel cell segment over the next years. One of their advantages is that they can work in reversible mode. However, in respect to durability, there are still some technical challenges. Although the quick development of experimental and modeling approaches gives insight into degradation mechanisms, an obligatory step that cannot be avoided is the performance of long-term tests. Taking into account the target for a commercial lifetime is 80 000 h [1], experiments lasting years are not acceptable for market needs. This work aims to develop accelerated stress tests (ASTs) for SOFCs by artificial aging of the fuel electrode via redox cycling, which follows the degradation processes of calendar aging (Ni coarsening and migration). The advantages of the developed procedure are that it offers a mild level of oxidation, which can be governed and regulated by the direct impedance monitoring of the Ni network resistance changes during oxidation/reduction on a bare anode sample. Once the redox cycling conditions are fixed and the anode/electrolyte sample is checked for cracks, the procedure is introduced for the AST in full-cell configuration. The developed methodology is evaluated by a comparative analysis of current voltage and impedance measurements of pristine, artificially aged, and calendar aged button cells, combined with microstructural characterization of their anodes. It can be applied in both fuel cell and electrolyzer mode. The results obtained in this study from the electrochemical tests show that the artificially aged experimental cell corresponds to at least 3500 h of nominal operation. The number of hours is much bigger in respect to the microstructural aging of the anode. Taking into consideration that the duration of the performed 20 redox cycles is about 50 to 60 working hours, the acceleration factor (AF) in respect to experimental timing is estimated to be higher than 60, without any damaging of the sample:

$$AF = t_{\text{long term test}} / t_{\text{AST bringing to the same degradation}} \quad (1)$$

The *i*-*V* curves obtained during redox cycling demonstrate well distinguished deterioration of the cell performance in comparison with the initial state (Fig. 1).

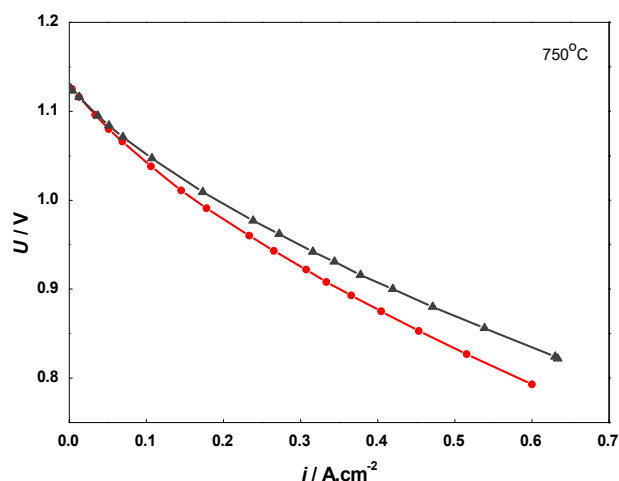


**Fig. 1:** Current-voltage ( $i$ - $V$ ) curves of: artificially aged cell before redox cycling ( $\blacktriangle$ ) and after 20 redox cycles ( $\bullet$ ).

This result shows that the selected approach is very promising for a large decrease in testing times for SOFCs.

#### Acknowledgements

The authors acknowledge the support of the Bulgarian Ministry of Education and Science under the: (i) Bulgarian National Recovery and Resilience Plan, Component "Innovative Bulgaria", Project № BG-RRP-2.004-0006-C02 "Development of research and innovation at Trakia University in service of health and sustainable well-being" and (ii) National Roadmap for Research Infrastructure 2017-2023 "Energy storage and hydrogen energetics (ESHER)", approved by DCM № 354/29.08.2017.

#### References

[1] A. Hagen, SOFC: Cell, stack and system level. In Fuel Cells: Data, Facts and Figures; Stolten, D., Samsun, R.C., Garland, N., Eds.; WILEY-VCH:Weinheim, Germany, 2016; ISBN 978-3-527-33240-3.

## EIS Analysis of PEDOT-Modified Electrodes – Stability, Thickness Distribution, and Non-Stationarity

Gyöző G. Láng<sup>a</sup>, Mária Ujvári<sup>a</sup>, Krisztina J. Szekeres<sup>a</sup>, Soma Vesztergom<sup>a</sup>

<sup>a</sup> *Institute of Chemistry, Eötvös Loránd University, Pázmány Péter sétány 1/A, H-1117 Budapest, Hungary, langgyg@chem.elte.hu*

The objective of this study was to electrochemically prepare and analyze electrodes that have been changed with poly(3,4-ethylenedioxythiophene) (PEDOT), both before and after undergoing overoxidation. The advantages of employing electropolymerization reactions for modifying electrode surfaces lie in the capacity to alter the characteristics of the polymer film by manipulation of the experimental circumstances, as well as the capability to customize the electrodes for particular purposes.

The systems were electrochemically characterized using cyclic voltammetry (CV) and electrochemical impedance spectroscopy (EIS). Based on the results, the impedance response of the overoxidized films significantly deviates from that of the freshly manufactured films. The declining capacitance of the double layer region and the rising charge transfer resistance indicate that the electrochemical activity of the film decreases during overoxidation, and the charge transfer process at the metal/film interface becomes more obstructed compared to pristine films. Furthermore, the electrochemical characteristics of the films exhibit changes over time following overoxidation, which suggests that the system is not in a stationary state.

The mechanical properties of the poly(3,4-ethylenedioxythiophene) layers and their resistance to the negative effects of overoxidation can be greatly enhanced by electrochemically depositing poly(bisphenol A) (poly(BPA)) onto its surface and within its pores, thereby combining the two polymers. This technique looks promising in terms of mechanical properties [1,2,3]. It is established that pure poly(BPA) exhibits low electrochemical conductivity and limited electrochemical activity [4]. Consequently, it was anticipated that the presence of poly(BPA) would have minimal impact on the electrochemical characteristics of the PEDOT layer, even following its overoxidation. The obtained results confirmed this expectation.

During the process of modeling the impedance response of the polymer modified electrodes, we faced two challenges: the uneven distribution of film thickness and the dynamic changes over time in the system. In order to minimize the impact of non-stationarity [5], we employed the four-dimensional (4D) analytical technique [6,7] to compute the impedances associated with different moments in time.

An important finding of this study is that the impedance responses of electrodes modified with PEDOT and poly(BPA)/PEDOT deviate from the expected purely capacitive behavior at low frequencies, as predicted by theoretical models. This deviation, known as frequency dispersion of low frequency capacitance, can be attributed solely to the uneven thickness of the film. The impedance model, which incorporates the film thickness distribution by assuming varied film thicknesses in various places based on SEM micrographs, accurately describes the impedance data both prior to and following overoxidation. This model allowed CNLS fitting the impedance function to the actual data to provide adequate values for the various parameters characterizing the polymer film electrodes.

### Acknowledgements

Financial support from the National Research, Development, and Innovation Office (NKFIH, grant nos. K129210, FK135375) is gratefully acknowledged.

## References

- [1] K.J. Szekeres, M. Ujvári, S. Vesztergom, G.G. Láng, *Electrochimica Acta* 391 (2021) 138975, doi: 10.1016/j.electacta.2021.138975
- [2] G.G. Láng, Experimental methods for the determination of stress changes at electrified solid–liquid interfaces, In: *Encyclopedia of Solid-Liquid Interfaces: Experimental and Theoretical Methods* (Vol.1), Elsevier, Amsterdam (2024). doi: 10.1016/B978-0-323-85669-0.00134-3
- [3] Conducting polymer composites containing iron oxide/hydroxide and their preparation using ferrate salt, international patent application, PCT/HU2022/050014, (Gyöző G. Láng, Krisztina J. Szekeres)
- [4] K.J. Szekeres, É. Fekete, M. Ujvári, S. Vesztergom, V.V. Kondratiev, G.G. Láng, *Russian Journal of Electrochemistry* 55 (2019) 1381-1390. doi: 10.1134/S1023193519110132.
- [5] Z. Stoykov, B. Savova, *Journal of Electroanalytical Chemistry* 112 (1980) 157–161. doi: 10.1016/S0022-0728(80)80016-7
- [6] Z. Stoykov, B. Savova-Stoykov, *Journal of Electroanalytical Chemistry* 183 (1985) 133-144. doi: 10.1016/0368-1874(85)85486-1
- [7] K.J. Szekeres, S. Vesztergom, M. Ujvári, G.G. Láng, *ChemElectroChem* 8 (2021) 1233-1250, doi: 10.1002/celec.202100093

# Disentangling the Capacitive Response of Single Crystal Pt Surfaces at the Onset of the Alkaline Hydrogen Evolution Reaction

Sheena Louisia<sup>a</sup>, Marc Koper<sup>a</sup>

<sup>a</sup> Leiden institute of Chemistry, Gorlaeus Laboratories, P.O. Box 9502, 2300 RA Leiden, The Netherlands, s.louisia@lic.leidenuniv.nl

The alkaline hydrogen evolution reaction (HER) offers a promising route toward the electrocatalytic production of clean hydrogen. Although less kinetically favoured than in acidic pH, alkaline conditions are more favourable to utilizing metals less precious and expensive than traditional Pt catalysts. It is therefore crucial we investigate what parameters at the electrode interface can be leveraged to optimized alkaline HER. In the presented work, we used electrochemical impedance spectroscopy (EIS) to interrogate the capacitive character and kinetics of charge transfer observed on Pt surfaces as a function of (1) applied potential, (2) cation concentration, and (3) step density. We focused our measurements to the hydrogen underpotential deposition ( $H_{UPD}$ ) potential region down to the onset of HER (**Fig. 1a**). Because measured in alkaline conditions, the kinetics of the electron transfer associated with hydrogen adsorption becomes much slower than the charging of the double layer. Occurring on a different timescale, these phenomena can thus be easily distinguished using EIS [1]. The double layer capacitance appears to decrease slightly as we approach the HER onset (**Fig. 1b**). Interestingly, Pt(111) seems to present little to no changes in the double layer capacitance with increasing cation concentration [2]. In contrary, the presence of 110 steps on the Pt(553) surface introduces a positive cation dependence for the double layer capacitance. The lower double layer capacitance observed on Pt(111) also suggests the interaction between H-covered Pt atoms and solvated cations varies between terrace and step sites. The implications of those interfacial differences observed between surface sites and cations on our understanding of the alkaline HER mechanism will be discussed here.

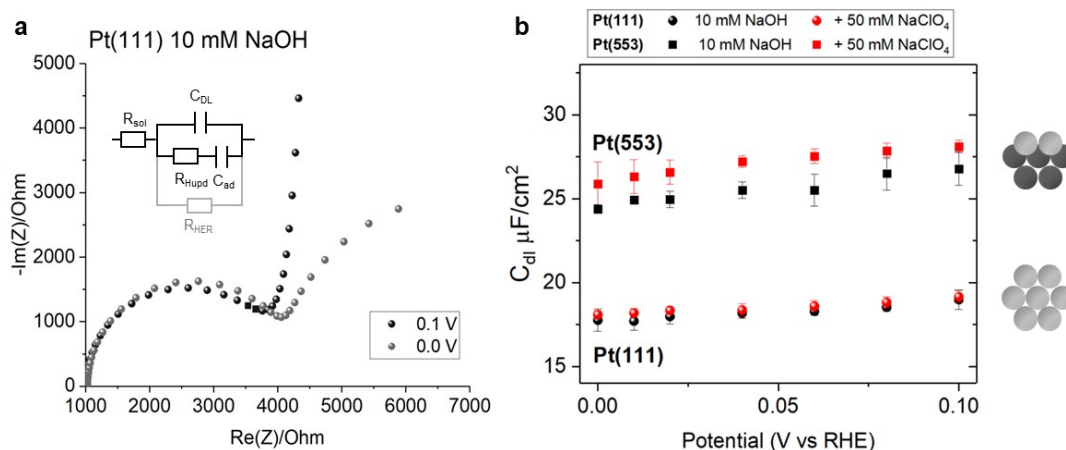


**Fig. 1.** (a) Different charge transfers are accounted for in the  $H_{UPD}$  potential region (0.1 V vs RHE) and at the onset of HER (0.0 V vs RHE) to fit the Nyquist plots measured for Pt(111) in 10 mM NaOH. (b) The double layer capacitance ( $C_{dl}$ ) obtained from fitting the EIS of Pt(111) and Pt(553) in 10 mM NaOH and 10 mM NaOH + 50 mM  $NaClO_4$  reveal different surface-electrolyte interactions.

## References

- [1] Schouten, K., Van Der Niet, M. & Koper, M. *Phys. Chem. Chem. Phys.* 12, 15217-15224 (2010).  
 [2] Goyal, A., Louisia, S., Moerland, P. & Koper, M. T. M. *JACS* (2024).

## Electrochemical Impedance Spectroscopy of Steels in Supercritical Water

Jan Macák<sup>a</sup>, David Dašek<sup>a</sup>, Jaromír Valtr<sup>a</sup>, Petr Roztočil<sup>a</sup>, Mariana Arnoult-Růžičková<sup>a</sup>, Petr Sajdl<sup>a</sup>, Radek Novotný<sup>b</sup>, Michal Novák<sup>a,b</sup>

<sup>a</sup> Power Engineering Department, University of Chemistry and Technology, Technická 3, 16628, Prague 6, Czech Republic, macakj@vscht.cz

<sup>b</sup> JRC-IET, Westerduinweg 3, NL-1755LE, Petten, the Netherlands

Among the Generation IV nuclear reactor concepts, the supercritical water (scw) cooled reactor (SCWR) occupies an important place. SCWR provides the advantage of significantly higher thermal efficiency compared to current reactor types (Generation II and III). However, the higher operating parameters impose a much higher demand on the corrosion resistance of structural materials, especially the fuel cladding material. One of the objectives of the international ECC SMART project [1] is to test the behaviour of novel materials and to suggest a potential substitute for currently used zirconium alloys. Corrosion tests are performed in scw test loop at 380°C and 500°C and 25MPa [2]. Besides standard after-exposure testing, electrochemical methods are used to obtain in-situ corrosion data. Previous work [3] has confirmed the feasibility of such measurements and good agreement between electrochemical corrosion data and data obtained by other methods. The experimental methodology consists of a sequence of EIS measurements over time. From the impedance spectra, the faradaic resistance is evaluated, which is a fundamental parameter determining the instantaneous corrosion rate. By converting to corrosion current and integrating the time dependence, integral corrosion data can be obtained which are directly comparable to the results of weight gain / loss measurements.

An example of a typical impedance spectrum is shown in Figure 1. In the high frequency region is the bulk response of the environment (supercritical water), in the middle and low frequencies the response of the working electrode. Data fitting was performed using equivalent circuit depicted in Fig. 1 (right).

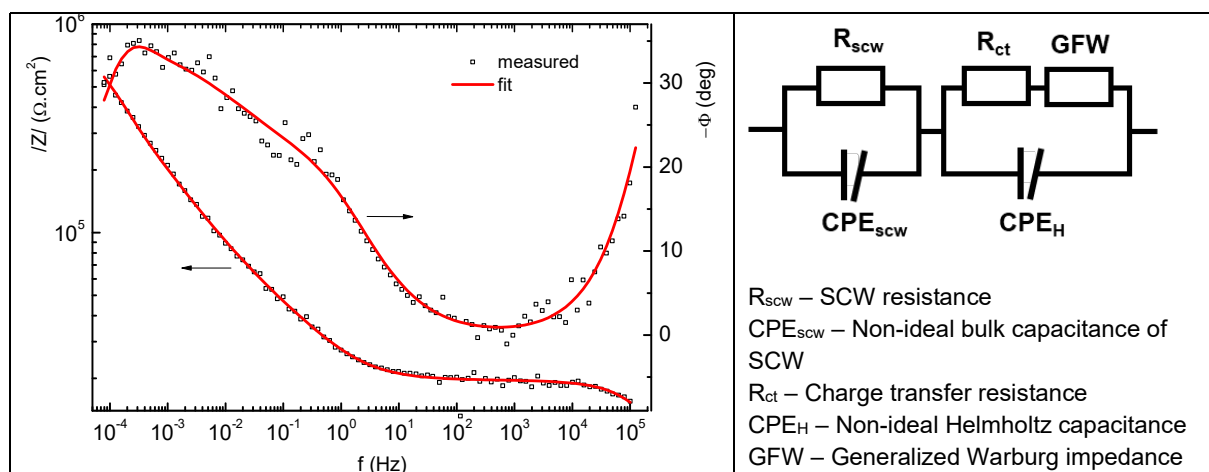


**Fig. 1:** Bode plot of impedance of 800H steel. Measured in supercritical water at 500°C, 25MPa and 150ppb of  $O_2$  after 705 hours of exposure (left). Equivalent circuit used for fitting (right).

The impedance response expresses the effect of mass transfer in the interaction of steel with scw. The corrosion rate of the 800H steel in supercritical water is controlled by diffusion of oxygen ions across the oxide layer formed on the surface. Finite-length Warburg element in generalized form was used, impedance of which is:

$$Z_{GFW} = R_{dif} \cdot \frac{\tanh(Tj\omega)^\varphi}{(Tj\omega)^\varphi} \quad (1)$$

where  $R_{dif}$  is diffusion resistance,  $T$  and  $\varphi$  are Warburg coefficient and exponent, respectively. Polarization resistance, which is used as the main corrosion parameter, was calculated as the sum of diffusion and charge transfer resistances:

$$R_p = R_{dif} + R_{ct} \quad (2)$$

Impedance data helped to explain the deviation of the temperature dependence of the corrosion rate from the Arrhenius equation around the critical point and the effects of dissolved oxygen concentration and surface treatment on the corrosion rate.

### Acknowledgement

This work received funding from EU Horizon 2020 Programme of EURATOM (H2020-NFRP-2019/2020) under grant agreement n° 945234 (ECC-SMART). Part of this work was supported from the grant of the Specific university research –MSMT A1\_FTOP\_2023\_001.

### References

- [1] Joint European Canadian Chinese Development of Small Modular Reactor Technology project (ECC SMART) <https://ecc-smart.eu>
- [2] J. Valtr J., P. Roztočil, D. Dašek, R. Mušálek, F. Lukáč, J. Klečka, M. Janata, M. Arnoult-Růžičková, E. Mištová, L. Jelínek, P. Sajdl, J. Macák. Measurement system for in-situ estimation of instantaneous corrosion rate in supercritical water, *The Journal of Supercritical Fluids*. 204 (2024) 106091.
- [3] J. Macák, R. Novotný, P. Sajdl, V. Bystrianský, L. Tůma, M. Novák. In-situ electrochemical impedance measurements of corroding stainless steel in high subcritical and supercritical water. *Corrosion Science* 150 (2019) 9-16.



## A Noise Based Approach to Constant Phase Behaviour; Is there such a Thing as Charge Transfer Resistance?

Gábor Mészáros

*Institute of Materials and Environmental Chemistry, HUN-REN Research Centre for Natural Sciences, Magyar tudósok körútja 2., H-1117 Budapest, Hungary, meszaros.gabor@ttk.hu*

One of the most frustrating problems in electrochemical impedance analysis is the appearance of the so called constant phase behaviour, characterized by a phase angle different from 0, +/-45 or +/-90 degrees. The problem with such a constant phase element (CPE) is that no physical relevance can be attributed to it, moreover the dimensions of the obtained parameters are also questionable. The usual explanation to the existence of such behaviour is the dispersion of the time constants present in the system, due to the structure and/or inhomogeneity of the electrode surface, resulting different reaction rate, diffusion control, solution drop, double layer capacitance in different points of the electrode. However, when we get to the point when we have to set up an equivalent circuit, all the CPE behaviour is compressed into the element representing the double layer capacitance, keeping an ideal charge transfer resistance, Warburg impedance and solution resistance. The reason is that most of the researchers applying EIS are interested in evaluating reaction rates and for that we desperately need an ideal charge transfer resistance. On the other hand, physicists or physical chemists are often interested rather in finding interfacial capacitances than reaction rates. For them a CPE model for the double layer capacity is completely useless.

On the other hand, if we approach the phenomenon from the point of view of shot noise – which must be the dominant one in the high frequency region – a CPE behaviour means an increase in the real part of the admittance with increasing frequency which, taking account the Schottky formula, implies that the apparent reaction/exchange rate increases with increasing frequency. The classical shot noise theorem and also the concept of charge transfer resistance suppose that the elementary charge transfer step take place in a random and independent way. The increase in the rate with increasing frequency can be explained with the existence of strongly correlated elementary charge transfer step pairs where a charge transfer step is followed a correlated charge transfer step to the backward direction. The phenomenon must have a mechanistic reason, e.g. after a charge transfer step the surface must locally relax. As long as the relaxation does not take place completely there is a high probability of a correlated backward step.

In the present work an attempt is made to keep an ideal element for the double layer capacity and to apply a frequency dependent element in place of the charge transfer resistance, and hopefully open a constructive discussion in the meeting.

## Non-Stationary Impedance: the Case of the Volmer-Heyrovský Corrosion Reaction

Nicolas Murer, Jean-Paul Diard, Bogdan Petrescu

BioLogic SAS, 4 rue de Vaucanson, 38170 Seyssinet-Pariset, France, nicolas.murer@biologic.net

In this work, a corrosion mechanism without mass transport limitation is considered, involving the Volmer-Heyrovský [1-3], and references therein] two-step proton reduction reaction with one adsorbate and a direct oxidation of the metal. The various reaction rates are time-dependent via the evolution of the free corrosion potential.

A theoretical expression of the non-stationary potential is calculated by solving a differential algebraic equation system, where the differential equation is the production rate of the adsorbed species and the algebraic equation is setting a zero net current.

Using non-stationary impedance expressions, time-variant Nyquist impedance graphs (Fig. 1) and the time evolution of the various resistances involved in the Faradaic impedance expressions (transfer, adsorption, polarization) (Fig. 2) can be plotted.

Finally, it is shown that an electrical equivalent circuit with time-dependent parameters can be used to fit the time-variant data (Fig. 3). A similar approach was conducted in the case of a redox reaction with mass transport limitation where the electroactive species concentration changes with time [4].

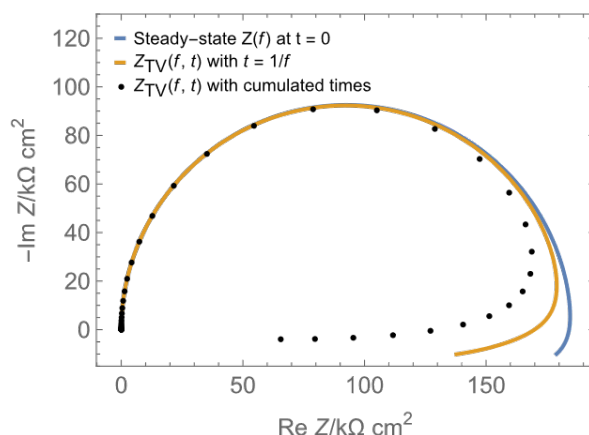


**Fig. 1:** Simulated impedance graphs of a system undergoing corrosion following a Volmer-Heyrovský corrosion mechanism without mass transport limitation, for a given set of kinetic parameters.

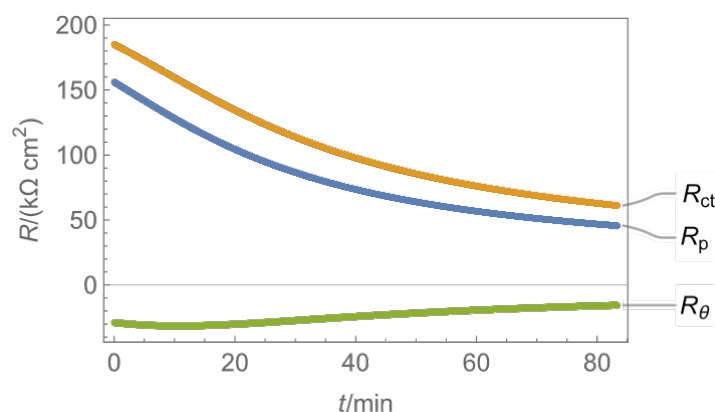


**Fig. 2:** Simulated time evolution of the various resistances composing the impedance of a system undergoing corrosion through a Volmer-Heyrovský corrosion mechanism without mass transport limitation, for a given set of kinetic parameters.

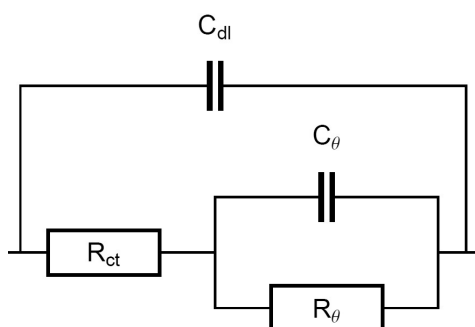


**Fig. 3:** Electrical equivalent circuit that can be used to model the impedance of a system undergoing corrosion following a Volmer-Heyrovsky corrosion mechanism.

### References

- [1] J. Heyrovský, *Rec. Trav. Chim.*, 46 (1927) 582.
- [2] T. Erdey-Gruz and M. Volmer, *Z. Physik. Cl-rem.*, A 150 (1930) 203.
- [3] J. Huang, *ChemRxiv*. 2023; doi:10.26434/chemrxiv-2023-t26wg. This content is a preprint and has not been peer-reviewed.
- [4] N. Murer, J.-P. Diard, and B. Petrescu, *J. Electrochem. Soc.*, 170 (2023) 126506

## Analysis of Carbohydrates on Charged Surfaces

Veronika Ostatná, Tatiana Galicová, Hana Černocká,

<sup>a</sup> *Department of Biophysical Chemistry and Molecular Oncology, Institute of Biophysics CAS, v.v.i., Královopolská 135, 612 00 Brno, Czech Republic, ostatna@ibp.cz*

In general, carbohydrates do not contain any redox centers that could have provided well-measurable electrochemical signals and therefore saccharides are mainly defined as electrochemically inactive compounds. However, polysaccharides with sulfated moieties and those with protonated amino groups produce an electrocatalytic chornopotentiometric peak similar to peak H of proteins [1]. The formation of the peak was attributed to the polymer character of the polysaccharide and the ability of some groups with an exchangeable proton (amino, sulphhydryl, ...) to be involved in the catalytic hydrogen evolution reaction. However, most amino groups of carbohydrates are acetylated and cannot give protons to the catalytic hydrogen reaction, so they are electrochemically inactive. In addition to monitoring the electron transfer of redox and catalytic reactions, surface-associated processes such as adsorption, desorption, and reorientation of carbohydrates can be studied. Carbohydrates with many hydroxyl groups form a hydrogen bond network affecting the water arrangement around them [2]. Changes in water arrangements strongly influence carbohydrate interfacial behavior at charged interfaces, enabling for instance, analysis of different fragments of hyaluronic acid [3].

### Acknowledgement

This research was supported by the Czech Science Foundation by project No. 22-26590S.

### References

- [1] E. Paleček, J. Tkáč, M. Bartošík, T. Bertók, V. Ostatná, J. Paleček, *Chemical Reviews* 115 (2015), 2045.
- [2] T. Galicová, S. Hasoň and V. Ostatná, *Bioelectrochemistry* 152, (2023), 108457.
- [3] E. Švecová, V. Ostatná, L. Fojt, M. Hermannová, V. Velebný and F. Ondreáš, *Carbohydrate Polymers* 277, (2022),118831

## Analysis of Quasi-Reversible CVs and dEIS Data: Transformation to Potential-Program Independent Forms

Tamás Pajkossy

*Institute of Materials and Environmental Chemistry, Research Centre for Natural Sciences,  
H-1117 Budapest, Magyar tudósok körútja 2, Hungary, pajkossy.tamas@ttk.mta.hu*

Dynamic electrochemical impedance spectroscopy, dEIS, comprises repetitive impedance spectrum measurements while slow scan-rate voltammetry is running. Its main virtue is the short measurement time, reducing the danger of contamination of the electrode surface. To further the use of dEIS, we have recently elaborated a set of theories aimed at the related data processing for three groups of fundamental electrode reactions: diffusion-affected charge transfer, charge transfer of surface-bound species, and adsorption-desorption. These theories yielded equations by which the voltammograms can be transformed to potential program invariant forms, allowing an easy calculation of the system parameters like rate coefficients; similar equations have been derived for the potential dependence of equivalent circuit parameters obtained from the impedance spectra. These derivations have also been presented in a single, unified one [1]. An example is shown in the figure below: From a set of “quasi-reversible” CVs taken at varied scan-rates  $\nu$ , two scan-rate independent, hysteresis-free functions can be calculated. One of them is the diffusion-free polarization curve,  $j_{\text{inf}}(E)$ , the other is the semiintegrated form of the reversible CV,  $M_{\text{rev}}(E)$ .

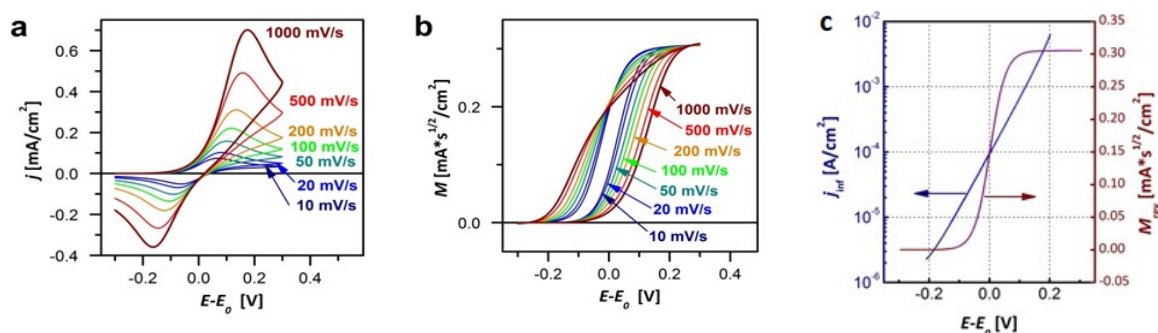


**Fig. 1:** Simulated CVs of a diffusion affected charge transfer reaction with varied scan rates (a), their semiintegrals (b), and the calculated  $j_{\text{inf}}$  and  $M_{\text{rev}}$  functions (c). Simulation parameters:  $D_{\text{red}}=D_{\text{ox}}=10^{-5}$  cm<sup>2</sup>/s,  $c_{\text{red}}=10^{-6}$  mol/cm<sup>3</sup>,  $c_{\text{ox}}=0$  mol/cm<sup>3</sup>,  $E_0=0$ ,  $k_0=0.001$  cm/s,  $\alpha=0.5$ .

The theory is recommended to evaluate electrode kinetic measurements, particularly when the potential dependence of rate coefficients is under study. Implications to electroanalytical chemistry are also involved.

### Reference

1. T. Pajkossy, *J. Phys. Chem. Lett.*, 14 (2023) 10599

## EIS on All Solid State Li-Ion Batteries with Halide Based Electrolyte: an Insight on the Battery Condition during Operation

Paolo Piccardo<sup>a</sup>, Roberto Spotorno<sup>a</sup>, Han-Xin Mei<sup>a</sup>, F. Pezzana<sup>b</sup>

<sup>a</sup> *Department of Chemistry and Industrial Chemistry, University of Genoa, Via Dodecaneso 31, 16146 Genoa, Italy; paolo.piccardo@unige.it*

<sup>b</sup> *Phase Motion Control S.p.A., Via Luigi Cibrario, 4, 16154 Genoa, Italy*

All-solid-state Li-ion batteries are a fascinating and extensively researched topic due to their potential as safe and efficient alternatives to current state-of-the-art Li-ion batteries. The use of halide-based electrolytes has opened new avenues, enabling the development of innovative devices with promising, though not yet market-ready, performance. However, the overall resistance remains high, potentially affecting energy density. Additionally, experiments have shown the influence of temperature and a self-healing property when Li-metal is used as the anode. While graphite-based anodes are also of interest, they face durability challenges.

Given the inherent difficulty in continuously monitoring the evolution of battery layers, Electrochemical Impedance Spectroscopy (EIS) is the most suitable and effective tool for real-time information gathering.

This communication is an initial step aimed at stimulating discussion on this cutting-edge frontier of Li-ion batteries.

### References

- [1] Han-xin Mei, Paolo Piccardo, Alessandro Cingolani, Roberto Spotorno, Unconventional solid-state electrolytes for lithium-based batteries: Recent advances and challenges, *Journal of Power Sources* 553 (2023) 232257
- [2] Han-xin Mei, Paolo Piccardo, Giovanni Carraro, Marco Smerieri, Roberto Spotorno, Thin-film  $\text{Li}_3\text{InCl}_6$  electrolyte prepared by solution casting method for all-solid-state batteries, *Journal of Energy Storage* 72 (2023) 108244

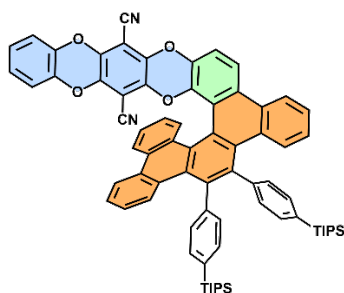
## Electrochemical Impedance of Organic Multiple Redox Sites

Lubomír Pospíšil,<sup>a,b</sup> Jan Hanus,<sup>b</sup> Michal Šámal,<sup>b</sup> Jiří Rybáček,<sup>b</sup> Václav Houska,<sup>b</sup> Irena G. Stará,<sup>b</sup> Ivo Starý<sup>b</sup>

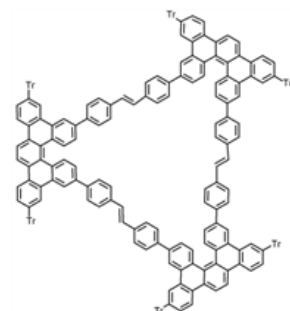
<sup>a</sup> J. Heyrovský Institute of Physical Chemistry, Czech Academy of Sciences, Czech Republic, [lubomir.pospisil@jh-inst.cas.cz](mailto:lubomir.pospisil@jh-inst.cas.cz)

<sup>b</sup> Institute of Organic Chemistry and Biochemistry Czech Acad. of Sciences, Czech Republic

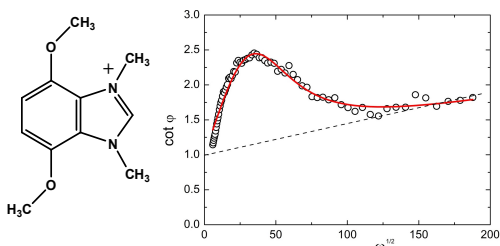
AC voltammetry and EIS are suitable methods conveniently complementing standard use of the cyclic voltammetry. We will show three examples of electrochemistry of organic compounds having multiple redox sites. Work on the first two examples is still in progress.



The first example is the identification of two different redox sites in an oxapentacene-helicene dyad. Synthesis of this new dyad is a part of a project searching for the helicene-based circularly polarised light (CPL) emitters. The application should lead for the construction of organic circularly polarised light-emitting diodes. AC voltammetry and the frequency dependence of the faradaic phase angle confirmed an EC mechanism in oxidation of the dyad.



The second example involves a triangular compound having in each corner the helicene structure. The connecting arms may or may not promote the electronic communication between three redox active helicenes. Voltammetric curves are rather drawn out and not suitable for resolution of redox steps. AC voltammetry shows that helicene redox centers have potentials 1.40 V, 1.47 V, and 1.56 V. Redox sites communicate electronically via linkers.



The last example is from published papers on the evaluation of dimerization EC processes [1,2]. Substituted benzimidazoles are primarily used in pharmacology. Benzimidazolium derivatives were considered as intermediates in the synthesis of compounds yielding upon irradiation the singlet fission effect. Cations upon reduction of imidazolium ring and subsequent oxidation could yield desired pair of chromophores. The application of EIS yielded the frequency dependence of the faradaic phase angle. The second order dimerization and heterogeneous ET rate constants were evaluated by a program written in Mathematica. Found values are  $k_{dim} \sim 5 \times 10^7 \text{ L.mol}^{-1}.\text{s}^{-1}$  and  $k^0 = 0.63 \text{ cm.s}^{-1}$ .

### References

- [1] Plutnar, J.; Hromadová, M.; Ramešová, Š.; Havlas, Z.; Pospíšil, L. Electron Transfer Mechanism of Substituted benzimidazoles: Dimer Switching, Oscillations and Search for Singlet Fission Properties. *J. Phys. Chem. C* **2017**, *121*, 963–9969.
- [2] Pospíšil, L.; Hromadová, M.; Sokolová, R.; Lanza, C. Kinetics of Radical Dimerization. Simple Evaluation of Rate Constant from Convolution Voltammetry and Faradaic Phase Angle Data. *Electrochim. Acta*, **2019**, *300*, 284–289.

## Deep Learning Algorithm, Based on Convolutional Neural Networks, for Equivalent Electrical Circuit Recommendation for Electrochemical Impedance Spectroscopy, and its Application to an All-Iron Battery

Fermín Sáez-Pardo<sup>a</sup>, Carles Escoms-Espert<sup>a</sup>, Juan José Giner-Sanz<sup>a</sup>, Valentín Pérez-Herranz<sup>a</sup>

<sup>a</sup> IEC group, Depto. Ingeniería Química y Nuclear, Universitat Politècnica de València, Camí de Vera s/n, Valencia 46022, Spain, fersaepa@etsii.upv.es

Electrochemical Impedance Spectroscopy (EIS) is ubiquitous in electrochemistry. The analysis of EIS spectra can be performed with 2 methodologies: using physical-mathematical models and using Equivalent Electrical Circuits (EECs). The physical-mathematical models, which are based on differential equations, provide the most complete analysis, however, this analysis requires advanced mathematical skills, which hinders their practical application. On the other hand, the analysis by EECs, which is based on selecting a physically sound EEC model, does not require advanced mathematical skills and still provides useful information about electrochemical systems [1]. Consequently, the EEC methodology is used more often than the physical-mathematical methodology (a search on 9 April 2024 in Google Scholar without filters for “electrochemical impedance spectroscopy equivalent electrical circuit models” yields 145000 results, whereas “electrochemical impedance spectroscopy mathematical models” yields 50000 results).

The most critical part of the EEC methodology is the EEC selection, which is generally based on previous knowledge of the electrochemical system and pattern recognition (e.g. a depressed semicircle in a Nyquist plot is related to a Constant Phase Element (CPE) in parallel with a resistive element). Until now, the (human) analyst has to make the selection just based on his/her expertise and literature. However, nowadays, new developments in image recognition driven by Artificial Intelligence (AI) open a new space of possibilities to help humans analyze EIS spectra. In this regard, the Convolutional Neural Network (CNN) algorithm is a promising algorithm able to classify images according to visual patterns. The CNN algorithm is a deep learning algorithm (i.e. an algorithm that generates its own feature space during the training process) consisting of 2 different parts: the convolutional and neural parts. The convolutional part extracts image features using the convolution operation. The convolutional part is followed by the dense neural part, which classifies the image according to the features extracted by the convolutional part. The CNN algorithm has been widely used in different areas such as medical image analysis, autonomous driving, astrophysics, among others; however, until now, only few works have applied the CNN algorithm to EIS pattern recognition [2].

In this panorama, the aim of this work is to develop a DL algorithm, based on CNNs, able to recognize visual patterns in the Nyquist plot of an EIS spectrum in order to recommend a plausible EEC for the spectrum.

To fulfill the aim of this work, we started with the database generated by Shan Zu et al. [3], which contains experimental EIS spectra obtained from scientific publications and labeled with the EEC selected by the authors of the original work (i.e. 5 types of EEC were considered). Then, the database of Shan Zu et al. was refined and used to generate an image database. Once the image database was complete, we used it to optimize the CNN architecture in 3 sequential stages: In the first stage, the convolutional architecture and activation function were optimized. In the second stage, the Initial Learn Rate (ILR) was optimized for the candidates



selected in the first step. In the third stage, the dense neural network architecture was optimized for the best convolutional architecture, activation function, and ILR combinations, identified in the previous steps.

As a result of this optimization process, we obtained a trained optimum CNN model, which achieved a test accuracy between 38.89% and 56.48% (95% confidence level), a 48.14% median test accuracy, and a maximum test accuracy of 61.11%. These results are better than the AI models based on Machine Learning proposed by Shan Zu et al. (48% maximum test accuracy) [3] and Zhaoyang et al. (57.0% maximum test accuracy) [4]. Finally, the trained optimum CNN model was used to suggest EEC models for EIS spectra of an all-iron battery.

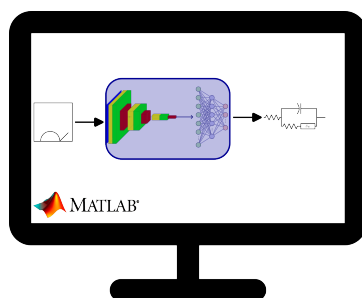


**Fig. 1:** Graphical abstract of this work. A Nyquist plot is fed into a Convolutional Neural Network (CNN) model. The CNN model extracts visual patterns and suggests an Equivalent Electrical Circuit (EEC) model.

### Acknowledgments

This work was funded by an “Ayuda a Primeros Proyectos de Investigación” project (PAID-06-23) of the research vice-rectorate of Universitat Politècnica de València. F.S.P. acknowledges the support of Universitat Politècnica de València through a predoctoral fellowship (PAID-01-22). J.J.G.S. is very grateful to the Ministerio de Ciencia e Innovación, to the Next Generation EU, and to the Agencia Estatal de Investigación, for their support by a Juan de la Cierva-Incorporación fellowship (IJC2020-044087-I) funded by MCIN/AEI/10.13039/501100011033 and by the European Union NextGenerationEU/PRTR.

### References

- [1] D. D. Macdonald, “Reflections on the history of electrochemical impedance spectroscopy,” *Electrochim Acta*, vol. 51, no. 8–9, pp. 1376–1388, 2006, doi: 10.1016/j.electacta.2005.02.107.
- [2] J. Schaeffer et al., “Machine Learning Benchmarks for the Classification of Equivalent Circuit Models from Electrochemical Impedance Spectra,” *J Electrochem Soc*, vol. 170, no. 6, p. 060512, 2023, doi: 10.1149/1945-7111/acd8fb.
- [3] S. Zhu et al., “Equivalent circuit model recognition of electrochemical impedance spectroscopy via machine learning,” *Journal of Electroanalytical Chemistry*, vol. 855, p. 113627, 2019, doi: 10.1016/j.jelechem.2019.113627.
- [4] Z. Zhao et al., “EIS equivalent circuit model prediction using interpretable machine learning and parameter identification using global optimization algorithms,” *Electrochim Acta*, vol. 418, p. 140350, 2022, doi: 10.1016/j.electacta.2022.140350.

## Electrochemical Impedance Spectroscopy Investigation of Vanadium Flow Battery Reactions at Glassy Carbon Electrodes

Varsha Sasikumar S. Pa<sup>a,b</sup>, Robert P. Lynch<sup>b,c</sup>, Maria Al-Hajji Safi<sup>b</sup>, D. Noel Buckley<sup>b,c</sup>, Andrea Bourke<sup>a,b</sup>

<sup>a</sup> Department of Electrical & Electronic Engineering, Technological University of the Shannon, Moylish Campus, V94 EC5T, Limerick, Ireland

<sup>b</sup> Department of Physics and Bernal Institute, University of Limerick, Castletroy, V94 T9PX, Limerick, Ireland

<sup>c</sup> Case Western Reserve University, 10900 Euclid Ave, OH 44106, Cleveland, United States

Flow batteries have been considered as a promising solution for flexible large-scale energy storage systems to tackle the problem of intermittency with renewable energy sources such as wind and solar. Among various flow battery systems, vanadium flow batteries (VFBs) have received a lot of attention particularly due to its advantages such as long cycle life with almost zero electrode and electrolyte degradation, safe and non-flammable aqueous electrolytes, zero cross contamination, scalability, and the ability to operate at reasonable temperatures. Carbon or graphite felts are commonly used as electrodes in VFBs due to their high electrical conductivity, chemical stability, and availability. The kinetics of the vanadium reactions is strongly affected by treatment (e.g., thermal, chemical, or electrochemical) of the carbon electrodes. [1,2]

We have previously reported that cathodic treatment enhances the kinetics of the positive ( $V^{IV}/V^V$ ) electrode but inhibits the kinetics of the negative ( $V^{II}/V^{III}$ ) electrode, while anodic treatment inhibits the kinetics of the positive electrode but enhances the kinetics of the negative electrode. [3-5] Recently we showed that the electrochemical activity of the  $V^{IV}/V^V$  and  $V^{II}/V^{III}$  redox reactions in highly acidic vanadium electrolytes at electrochemically treated glassy carbon electrodes is also affected by the pH of the treatment electrolyte. [6,7] The activities of glassy carbon electrodes towards both the  $V^{IV}/V^V$  and  $V^{II}/V^{III}$  redox reactions increase with increasing pH of the treatment electrolytes. The kinetic rates for both the  $V^{IV}/V^V$  and  $V^{II}/V^{III}$  redox reactions on these electrodes were measured and compared using cyclic voltammetry (CV) and electrochemical impedance spectroscopy (EIS). This work has resulted in some interesting EIS results.

In this presentation, we will compare these EIS results of variously pretreated glassy carbon electrodes for both the  $V^{IV}/V^V$  and  $V^{II}/V^{III}$  redox couples.

### References

- [1] D.N. Buckley, Flow Batteries: From Fundamentals to Applications, Edited by. C. Roth et al., Wiley-VCH, Chapter 24, (2023) ISBN 978-3-527-34922-7.
- [2] M. Zarei-Jelyani, M. Mohsen Loghavi, M. Babaiee, R. Eqra, *J. Appl. Electrochem.*, 54, (2024) 719.
- [3] A. Bourke, M. A. Miller, R. P. Lynch, X. Gao, J. Landon, J. S. Wainright, R. F. Savinell, D. N. Buckley, *J. Electrochem. Soc.*, 163 (2016) A5097.
- [4] A. Bourke, M. A. Miller, R. P. Lynch, J. S. Wainright, R. F. Savinell, D. N. Buckley, *J. Electrochem. Soc.*, 162 (2015) A1547.
- [5] A. Bourke, D. Oboroceanu, N. Quill, C. Lenihan, M. Alhajji Safi, M. A. Miller, R. F. Savinell, J. S. Wainright, V. Sasikumar, M. Rybalchenko, P. Amini, N. Dalton, R. P. Lynch, D. N. Buckley, *J. Electrochem. Soc.*, 170 (2023) 030504.
- [6] V. Sasikumar, R. P. Lynch, M. Alhajji Safi, D. N. Buckley, A. Bourke, *ECS Trans.*, 109, (2022) 107.
- [7] V. Sasikumar, R. P. Lynch, M. Alhajji Safi, M. Rybalchenko, D. N. Buckley, A. Bourke, *Meet. Abstr. MA2023-02* (2023) 2854.

## 3D Printed Impedimetric Sensing: A New Tool for Microfluidic Analysis

Táňa Sebechlebská<sup>a,b</sup>, Eva Vaněčková<sup>b</sup>, Federico Vivaldi<sup>c</sup>, and Viliam Kolivoška<sup>b</sup>

<sup>a</sup> Department of Physical and Theoretical chemistry, Faculty of Natural Sciences Comenius University in Bratislava, Mlynská dolina, Ilkovičova 6, 842 15 Bratislava, Slovakia, tana.sebechlebska@uniba.sk

<sup>b</sup> J. Heyrovsky Institute of Physical Chemistry of the Czech Academy of Sciences, Dolejškova 2155/3, 18223 Prague, Czech Republic

<sup>c</sup> Department of Chemistry and Industrial Chemistry, University of Pisa, Via Moruzzi 13, 56124 Pisa, Italy

In this study, we present a novel approach to fabricate an integrated platform for sensing the electrical properties of liquids and microfluidic channels using fused deposition modelling 3D printing (FDM-3DP). By combining electrically conductive and insulating filaments, we designed and manufactured a rectangular cell with parallel-plate electrodes for impedance measurements. We successfully demonstrated the platform's functionality by accurately measuring the conductivity of aqueous potassium chloride solutions and bottled water samples, as well as the permittivity of water/ethanol mixtures using a cost-effective measurement platform consisting of a function generator, ammeter, and voltmeter. The results obtained were in excellent agreement with reference values, validating the accuracy and precision of our 3D printed platform.

Furthermore, we extended the application of our platform to investigate the dimensions of 3D printed microchannels, fundamental components in microfluidic devices. By employing impedance measurements with an aqueous electrolyte, we determined the width of microchannels integrated into the platform. Through systematic manipulation of the extrusion multiplier in the 3D printing process, we achieved a minimum microchannel width of 80  $\mu\text{m}$ , showcasing the high-resolution capabilities of FDM-3DP for microfluidic applications.

This research demonstrates the potential of FDM-3DP for creating versatile platforms for sensing electrical properties of liquids and fabricating microfluidic devices with precise dimensions. The non-destructive impedimetric sensing approach we introduced offers a simple and cost-effective method for microanalytical applications, with potential implications for the manufacture of 3D printed lab-on-a-chip platforms.

### Acknowledgements

The authors are grateful to the Slovak Grant Agency APVV (grant number apvv-22-0150), Czech Science Foundation (grant numbers 21-13458S, 23-07292S) and Czech Academy of Sciences (grant number L200402251).

### References

[1] T. Sebechlebská, E. Vanečková, M. K. Choińska-Młynarczyk, T. Navrátil, L. Poltorak, A. Bonini, F. Vivaldi, V. Kolivoška. *Anal. Chem.*, 94 (2022) 14426.

## Reaction Kinetics in Water Electro-Oxidation Addressed by Impedance Spectroscopy for Redox-active NiFe Oxyhydroxides

Subhasis Shit<sup>a</sup>, Holger Dau<sup>a</sup>

<sup>a</sup> Department of Physics, Freie Universität Berlin, Arnimallee 14, 14195 Berlin, Germany, e-mail: subhasis.electrochem@gmail.com

Water oxidation, the oxygen evolution reaction (OER), is crucial in the production of ‘green hydrogen’ and further non-fossil fuels. NiFe-based oxyhydroxides are one of the most promising transition-metal based OER electrocatalysts, with especially facile (electro)synthesis routes [1]. In spite of many seminal investigations, crucial kinetic-mechanistic aspects are still insufficiently understood. One major knowledge gap that persists for NiFe and also other electrocatalyst materials is the detailed (quantitative) understanding of the relationship between electrochemical impedance spectroscopy (EIS) data and the atomistic events of the electrocatalytic process. Typically, equivalent circuit models (ECMs) are used to analyse the EIS output of a system; however, the correlation between the circuit elements and specific processes at atomistic level has often remained in the dark [2].

We fabricated a series of NiFe catalyst films with varying Ni:Fe ratios and performed EIS in 1.0 M KOH at varied potentials. The EIS data were analysed using an ECM with two R-C loops, describing the redox transition of the metal centers and the water oxidation catalysis. Operando UV-vis and X-ray absorption spectroscopy (XAS) experiments facilitated development of an informative ECM model and correlation to chemical events and reaction kinetics.

The following results support our understanding of water oxidation by NiFe-based catalysts: (i) there is a V-shaped relationship between water oxidation activity of NiFe film and its relative Fe content relating to a specific resistance value,  $R_{\text{cat}}$  [3]; (ii) Fe partially suppresses the redox transition in Ni centers, as indicated by  $R_{\text{ox}}$ -values [4]; (iii) the rate of Ni reduction during catalysis competes with Ni reoxidation, indicated by similar time constants (reciprocal rate constants) for metal center oxidation and catalysis [1,3]; and (iv) interestingly, the redox capacitance ( $C_{\text{ox}}$ ) increases with increasing potential in the catalytic region, indicating that another redox transition (different than the one associated with typical Ni oxidation) is likely to occur in this region (in line with previous spectro-electrochemical investigations on the NiFe system [5], which however were not stringently interpreted in this sense).

In conclusion, the parameters of the components in ECM can be correlated with the chemical processes that occur during water oxidation. We believe that the concepts here developed for redox-active NiFe materials for OER electrocatalysis may be relevant also for a broader class of electrocatalyst materials.

### References

- [1] S. Loos, I. Zaharieva, P. Chernev, A. Lišner, H. Dau. *ChemSusChem*, 12 (2019) 1966.
- [2] S. Shit, S. Ghosh, S. Bolar, N. C. Murmu, T. Kuila. *J. Electrochem. Soc.*, 167 (2020) 116514.
- [3] M. Görlin, P. Chernev, J. F. Araújo, T. Reier, S. Dresch, B. Paul, R. Krähnert, H. Dau, P. Strasser. *J. Am. Chem. Soc.*, 138 (2016) 5603.
- [4] D. González-Flores, K. Klingan, P. Chernev, S. Loos, M. R. Mohammadi, C. Pasquini, P. Kubella, I. Zaharieva, R. D. L. Smith, H. Dau. *Sustainable Energy Fuels*, 2 (2018) 1986.
- [5] R. D. L. Smith, C. Pasquini, S. Loos, P. Chernev, K. Klingan, P. Kubella, M. R. Mohammadi, D. Gonzalez-Flores, H. Dau. *Energy Environ. Sci.*, 11 (2018) 2476.

# Rotating Fourier Transform Applied to Electrochemical Impedance Spectroscopy: New Opportunities for Low-Frequency Measurements

Roberto Spotorno<sup>a</sup>, Daria Vladikova<sup>b,c</sup>, Paolo Piccardo<sup>a</sup>

<sup>a</sup> Department of Chemistry and Industrial Chemistry, University of Genoa, via Dodecaneso 31, 16146, Genoa, Italy, Roberto.Spotorno@unige.it

<sup>b</sup> Institute of Electrochemistry and Energy Systems – Bulgarian Academy of Sciences, 10 Acad. G. Bonchev, 1113 Sofia, Bulgaria

<sup>c</sup> Institute for Sustainable Transition and Development – Trakia University, Students Campus, 6000 Stara Zagora, Bulgaria

Electrochemical impedance spectroscopy is a powerful tool for analyzing electrochemical systems. It is particularly exploited in the fields of corrosion, energy storage and conversion. In this method, a small electrical perturbation is applied to the system to be analyzed and the response is observed. The perturbation can take the form of a sinusoidal potential/current wave with a specific frequency. The Fourier transform (FT) is commonly used to analyze the response of the system at different frequencies. It is a mathematical operation that establishes the link between the time and frequency domains:

$$X(\omega) = \frac{1}{NT} \int_0^{NT} x(t) \sin(\omega t) dt$$

where  $x(t)\sin(\omega t)$  describes the signal,  $\omega$  is the frequency,  $NT$  is the integration time. The FT allows good filtering of the random noise that often affects electrochemical measurements. However, its application requires the assumption that the system under investigation is in a steady state since, according to the traditional interpretation, impedance is not defined as a time-dependent quantity and therefore there should be no impedance out of stationary conditions. This is due to the poor filtering of the aperiodic noise by the Fourier transform.

In practice, the presence of aperiodic noise leads to drifts of the measured output signal (Figure 1a) which in turn causes deformation of the recorded spectrum (Figure 1b) especially at low frequencies, resulting in a source of data misinterpretation.

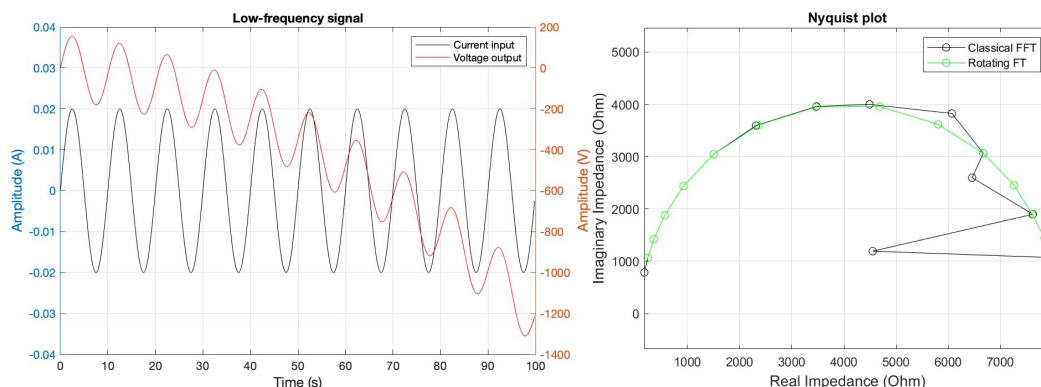


**Fig. 1:** a) difference between perturbation (current) and response (voltage) when the system is non-stationary; b) impedance spectrum calculated using FT and RTF

To limit such effect, when possible, it is good practice to wait for the system to stabilize before starting the impedance characterization. An alternative is to keep the measurement short by cutting off the lowest frequencies where the acquisition of each data point can take several minutes. It should be noted that such practices

cause the loss of information about the stabilization time and the low frequencies at which interesting phenomena occur.

In 1980, prof. Stoynov published a short communication about the instrumental error in impedance measurements of non-steady-state systems [1] and introduced, in 1985, the four-dimensional analysis [2], a method based on the acquisition of subsequent impedance spectra recording the measurement time of each data point. By treating the measured points using iso-frequency splines it is possible to extrapolate the instantaneous impedance spectrum, corrected by the deformations introduced by the non-stationary conditions.

The above researches led prof. Stoynov to the formulation of the Rotating Fourier transform (RFT), an elegant solution to the issues of non-stationary impedance, solving the problem at its root. It is basically an extension of the classical FT, which performs multiple integration in the phase domain and thus allows complete filtering of the aperiodic noise:

$$X(\omega) = \frac{1}{2\pi N} \int_{\varphi}^{\varphi+2\pi N_1} \int_{t_0}^{t_0+N_0 T} x(t) \sin(\omega t) dt d\varphi$$

where  $t_0$  is the initial phase of the first integration and  $\varphi$  is the initial phase of the following ones [3].

In this talk, the principle and application of the RFT for the calculation of electrochemical impedance will be presented with emphasis on properties discovered during the development of this method.

#### References

- [1] Z. Stoynov, B. Savova, J. Electroanal. Chem. 112 (1980) 157.
- [2] Z.B. Stoynov, B.S. Savova, J. Electroanal. Chem. 183 (1985) 133.
- [3] Z.B. Stoynov, Electrochimica Acta, 37 (1992) 2357.

## Validation and Reconstruction of Impedance Data – Combining Measurement Model and ZHIT Algorithm

Werner Strunz, Alexander Krimalowski

Zahner-Elektrik GmbH & Co KG, Thuringerstr.12, D-96317 Kronach, Germany,  
werner.strunz@zahner.de

Over the last decades, Electrochemical Impedance Spectroscopy (EIS) has established itself as an ideal analytical tool to investigate various systems of theoretical as well as of technical relevance. The broad applicability of EIS is based on its wide frequency span, ranging from about  $10^{-5}$  to  $10^7$  Hz, as well as the impedance, covering ca.  $10^{-6}$  to  $10^{12}$   $\Omega$ . Thus, it is not surprising that EIS plays a dominant role in the investigation of technical relevant systems like batteries, fuel cells, solar cells, or coated metals.

One major disadvantage of EIS is caused by the investigation under stimulation, i.e., battery systems are usually measured under charging/discharging conditions, solar cells under illumination and coated metals while they are taking up an electrolyte solution.

All these situations may lead to systems changing their state during the measurement. This is a radical violation of the stability criteria for EIS, which state that the device under test must not change during the measurement. Since the recording of each frequency data point requires a certain amount of time, different systems are observed between the beginning and the end of the measurement.<sup>[1]</sup>

In general, the evaluation of impedance spectra may be complicated by different detrimental contributions. Depending on the system, typical error contributions may apply, such as mutual induction, parasitic reactances, or electromagnetic interference. All of these can be considered more or less “simple” artifacts, but must be detected and corrected during the evaluation.

Furthermore, a significant complication comes from the large time scales of EIS and may not be visible in a spectrum: the measurement time increases dramatically when going from high to low frequencies. This may induce a significant system change during the measurement, at least for the lower frequency part of the spectrum.

Compared to, for example, time domain techniques, EIS offers a unique feature allowing a check for consistency on a measured data set: while in the time domain any data point is a real valued point, an EIS data point is a complex valued point, i.e., consists of a real and an imaginary part, both of which are strongly correlated. Therefore, the real part of a complex number can be calculated from the imaginary part and vice versa (Kramers Kronig Integral Transform, KKIT).

As a consistency check, two relevant algorithms are compared which enable the reliable detection of artifacts within an impedance spectrum. The first algorithm – the so-called Measurement Model – validates a spectrum by modulating the recorded spectrum by a sum of exponential functions which fulfils the KKIT conditions.<sup>[2-4]</sup>

The other algorithm is known in the literature as the ZHIT algorithm and also allows for the detection of artifacts. Moreover, ZHIT can reconstruct causal spectra from drift affected data, as it is a true descendant of the KKIT. This involves an integral term which allows to calculate drift affected data points (present in the low frequency) from the measured high frequency data points, as the latter are commonly not affected by drift effects.<sup>[5-8]</sup>

Comparing these two algorithms in more detail, it can be found that the ZHIT algorithm calculates the impedance from the phase shift, with the main contribution coming from the integral of the phase shift. In addition, a smaller correction term is

added resulting from the slope of the phase shift at each frequency point. However, this part is affected by an error increasing with the slope at each frequency. This is often the case for low-impedance systems, when inductive behavior merging into capacitive behavior, e.g., in batteries or fuel cells in the higher-frequency part of the spectrum.

In contrast, with the MM algorithm the utilization of "localized" exponential functions means that the functions no longer have an internal relationship between high and low frequencies, as it is for ZHIT.

In conclusion it can be stated that both algorithms should complement each other: The MM model is beneficial in the higher-frequency part, while in the low-frequency part the ZHIT allows for the detection and reconstruction of drift-affected data.

The application of both algorithms in combination is reported here.

### References

- [1] Stoynov, Z.; Savova-Stoynov, B. S. Impedance study of non-stationary systems: four-dimensional analysis *J. Electroanal. Chem.* 1985, 183, 133–144.
- [2] Agarwal, P.; Orazem, M.E.; García-Rubio, L. H. Measurement Models for Electrochemical Impedance Spectroscopy: I. Demonstration of Applicability *J. Electrochem. Soc.* 1992, 139, 1917.
- [3] Boukamp, B. A. A Linear Kronig-Kramers Transform Test for Impedance Data Validation, *J. Electrochem. Soc.* 1995, 142, 1885.
- [4] Schönleber, M.; Klotz, D.; Ivers-Tiffée, E. A Method for Improving the Robustness of linear Kramers-Kronig Validity Tests *Electrochim. Acta* 2014, 131, 20-27.
- [5] Ehm, W.; Kaus, R.; Göhr, H.; Schiller, C.A. The Evaluation of Electrochemical Impedance Spectra Using a Modified Logarithmic Hilbert Transform *Acta Chimica Hungarica* 2000, 137, 145.
- [6] Ehm, W.; Kaus, R.; Schiller, C. A.; Strunz, W. ZHIT - A Simple Relation between Impedance Modulus and Phase Angle, Providing a New Way to the Validation of Electrochemical Impedance Spectra, *Proceedings of the ECS, New Trends in Electrochemical Impedance Spectroscopy (EIS) and Electrochemical Noise Analysis (ENA)*, eds. F. Mansfeld, F. Huet. O.R. Mattos, Electrochemical Society, Pennington, NJ, vol. 2000-24 (2001) 1.
- [7] Schiller, C. A.; Richter, F.; Gülzow, E.; Wagner, N. Relaxation Impedance as a Model for the Deactivation Mechanism of Fuel Cells Due to Carbon Monoxide Poisoning *J. Phys. Chem. Chem. Phys.* 2001, 3, 2113.
- [8] <https://en.wikipedia.org/wiki/Z-HIT>



## Hydrogen Evolution at Constant Current, Accompanied by Time-Resolved Impedance Monitoring

Soma Vesztergom<sup>a</sup>, Ádám Kapdos<sup>a</sup>, Mária Ujvári<sup>a</sup>, Noémi Kovács<sup>a</sup>, Győző G. Láng<sup>a</sup>, Peter Broekmann<sup>b</sup>, Vitali Grozovski<sup>c</sup>

<sup>a</sup> MTA–ELTE Momentum Interfacial Electrochemistry Research Group, Eötvös Loránd University, Pázmány Péter sétány 1/A, 1117 Budapest, Hungary, soma.vesztergom@ttk.elte.hu

<sup>b</sup> Department of Chemistry, Biochemistry and Pharmaceutical Sciences, University of Bern, Freiestrasse 3, 3012 Bern, Switzerland

<sup>c</sup> Institute of Chemistry, University of Tartu, Ravila 14a, Tartu, 50411 Estonia

Cathodic hydrogen generation from unstirred dilute acids ( $2 < \text{pH} < 7$ ) often results in the vicinity of the electrode turning alkaline. Potential transients (Figure 1) recorded at constant current exhibit a sharp step at the moment of surface neutralisation, and the stepped chronopotentiograms convey important information with regard to the rate of both the electrode reaction and of transport.

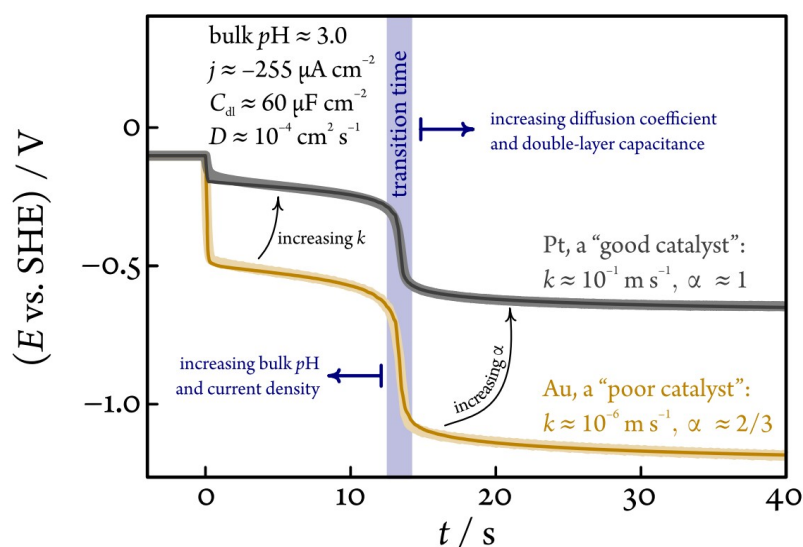


**Fig. 1:** Chronopotentiograms of cathodic hydrogen evolution at two different (Au and Pt) electrodes, recorded in a mildly acidic solution. Measured data are plotted in light colours; the dark curves show fits based on the model presented in this contribution.

Here we present a robust model that, although it contains only three variable parameters, can fit experimentally obtained chronopotentiometric curves remarkably well. The reaction rate and charge transfer coefficients obtained from the fitting can be combined into a  $\text{pH}$  dependent exchange current density of the hydrogen evolution reaction that can be used for the benchmarking of the catalytic activity of different electrode materials, while the obtained diffusion coefficient can be used in simple formulae to estimate the characteristic time of surface neutralisation and the rate of propagation of the neutrality front.

The presentation places special emphasis on the distorting effect of double layer charging on the obtained chronopotentiometric signal and discusses experimental means to record changes of the double-layer capacitance, as well as methods to account for capacitive charging effects by the application of semi-integration techniques.

## Accelerated *Ex-situ* Aging of Solid Oxide Fuel Cell Anode via Redox-Cycling Investigated by Differential Impedance Analysis

Daria Vladikova<sup>a,b</sup>, Roberto Spotorno<sup>c</sup>, M. Krapchanska<sup>a,b</sup>, B. Burdin<sup>a,b</sup>, P. Piccardo<sup>c</sup>

<sup>a</sup> Institute of Electrochemistry and Energy Systems – Bulgarian Academy of Sciences, 10 Acad. G. Bonchev, 1113 Sofia, Bulgaria, d.vladikova@iees.bas.bg;

<sup>b</sup> Institute for Sustainable Transition and Development – Trakia University, Students Campus, 6000 Stara Zagora, Bulgaria

<sup>c</sup> Department of Chemistry and Industrial Chemistry, University of Genoa, Via Dodecaneso 31, 16146 Genoa, Italy

Solid Oxide Fuel Cells (SOFC) have an important role in the emerging hydrogen technologies due to their advantage to operate in reversible mode with non-platinum catalysts and high tolerance towards hydrogen quality. However, additional work is needed to increase their durability. The work on life time improvement needs long term electrochemical tests for accumulation of reliable data which can be reduced by the introduction of Accelerated Stress Tests (AST). This work applies *ex-situ* accelerated artificial aging of SOFC anode (Ni/YSZ) by chemical redox cycling.

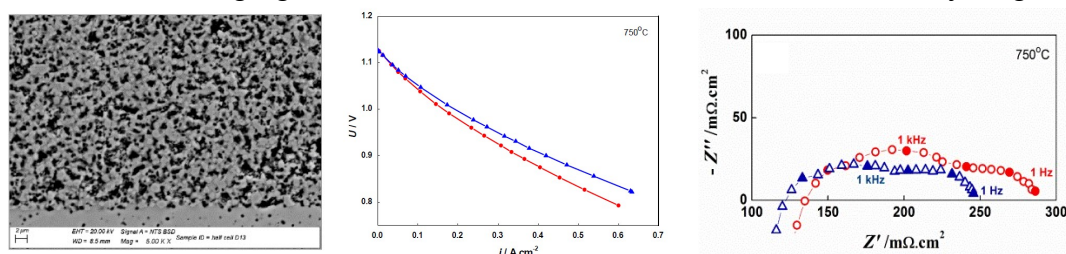


**Fig. 1:** Tested SOFC: SEM image after 20 redox cycles (left); pristine cell (blue) and after 20 cycles (red):  $i$ - $V$  curves (middle) and impedance diagrams under load of 0,28 A/cm (right).

The mild oxidation which prevents the system from irreversible degradation due to the cracking of the interface electrode/electrolyte (Fig. 1 left) was governed and monitored by specially developed impedance-based approach [1]. For quantitative evaluation of the accelerated degradation, current voltage ( $i$ - $V$ ) characteristics were measured periodically during redox cycling (Fig.1 middle). The impedance data in selected working points (Fig.1 right), recalculated as Area Specific Resistance (ASR), show that the biggest contribution in the ASR increase, caused by artificial aging, is coming from the polarization resistance (Table 1).

For deeper insight into the redox cycling, the impedance data were subjected to Differential Impedance Analysis (DIA) which is the kernel of the presented talk. DIA is an advanced technique for impedance data analysis, which introduces structural

**Table 1**

	ASR (mΩ·cm <sup>2</sup> )		Aging Factor, %
	0 Redox cycles	20 Redox cycles	20 Redox cycles
$ASR_{\Omega}$	58,7	63,5	8,2
$ASR_p$	59,8	42,5	24,5
$ASR_T$	92,8	106,0	14,2

approach [2], identifying both the structure and the parameters of the model (Eq. 1). Thus, it eliminates the necessity for initial working hypothesis and improves the information capability and objectivity of Electrochemical Impedance Spectroscopy.

$$\hat{M}[\hat{S}, \hat{P}] = \text{Str. Ident}[Z'_i, Z''_i, \omega_i] \quad (1)$$

The kernel of DIA is the scanning local analysis with a local estimator (LOM) moving along the analytical coordinate frequency with a scanning window of a single frequency point. The simplest LOM is a mesh of resistance  $R$  and capacitance  $C$  in parallel, extended with additive term  $Ad$ , connected in series. The procedure ensures parametric identification of the LOM parameters at every working frequency. The results are presented in Temporal plots (Fig. 2), where  $\nu = \lg \omega^{-1} = T_f$ .

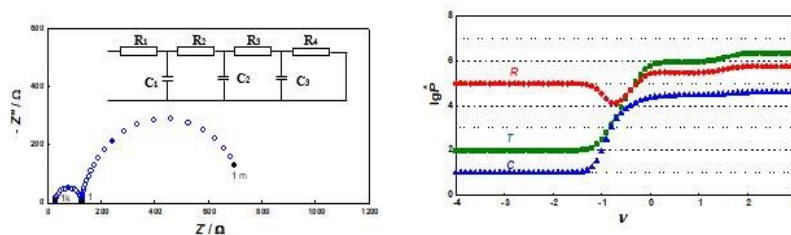


**Fig. 2:** Three step reaction – simulated data: equivalent circuit and complex-plane impedance diagram (left); temporal plots (right). The number of the plateaus, i.e. the regions where there is no frequency dependence of the LOM parameters' estimates determines the number of reaction steps.

While DIA recognizes models with lumped elements, the Secondary DIA recognizes frequency distribution. It is performed by differentiation of the logarithmic LOM parameters' estimates with respect to the logarithm of the frequency. The frequency analysis is represented as Differential Temporal Analysis.

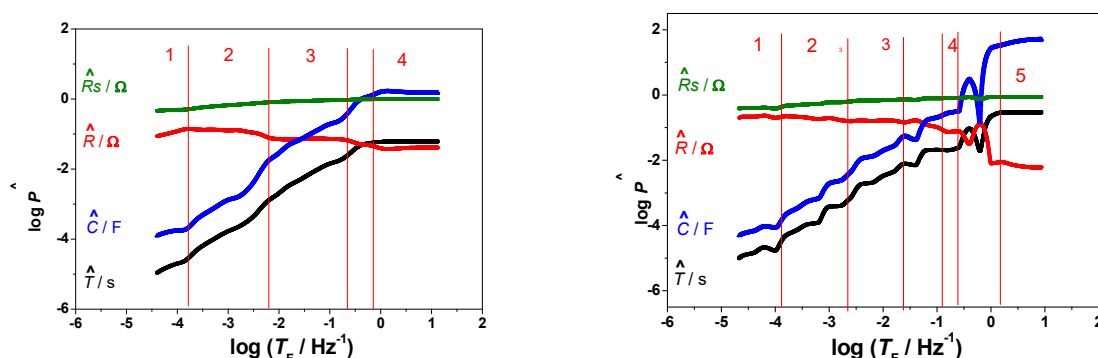


**Fig. 3:** Temporal plots of the Impedance diagrams presented in Fig. 1 (before redox cycling – left; after 20 cycles – right)

DIA was performed on impedance diagrams of button cell before and after 20 redox cycles at 0,28 A/cm<sup>2</sup> (Fig. 1 right) and 0,50 A/cm<sup>2</sup> load. As seen in Fig. 3, the temporal plots can be divided in several segments, corresponding to the number of steps taking part in the total process, with different level of distribution. The full DIA analysis, which will be presented in the talk, was derived by segmented Temporal and Differential Temporal Analysis, applying also the technique of the spectral transform.

### Acknowledgements

The authors acknowledge the support of the Bulgarian Ministry of Education and Science under the: (i) Bulgarian National Recovery and Resilience Plan, Component "Innovative Bulgaria", Project № BG-RRP-2.004-0006-C02 "Development of research and innovation at Trakia University in service of health and sustainable well-being" and (ii) National Roadmap for Research Infrastructure 2017-2023 "Energy storage and hydrogen energetics (ESHER)", approved by DCM № 354/29.08.2017.

### References

- [1] D.Vladikova, B. Burdin, A. Sheikh, P. Piccardo, M. Krapchanska, D. Montinaro, R. Spotorno, Accelerated Stress Tests for Solid Oxide Cells via Artificial Aging of the Fuel Electrode. *Energies*, 15 (2022) 3287. <https://doi.org/10.3390/en15093287>
- [2] Z. Stoynov, D. Vladikova, in *Encyclopedia of Electrochemical Power Sources*, edited by U. Garche (Elsevier, 2009) pp. 632.

## How Can we Bridge Experiments and Molecular Modelling in EIS?

Chao Zhang<sup>a</sup>

<sup>a</sup> Department of Chemistry – Ångström Laboratory, Uppsala University, Lägerhyddsvägen 1, BOX 538, 75121, Uppsala, Sweden

[chao.zhang@kemi.uu.se](mailto:chao.zhang@kemi.uu.se)

Molecular modelling is playing an increasingly important role in the mechanistic understanding and quantitative predictions of electrochemical systems [1]. Nevertheless, an enormous gap exists between experiments and molecular modelling when it comes to electrochemical impedance spectroscopy (EIS). Here, I will first introduce our recent progress in extracting materials properties that are relevant to EIS from molecular modelling, including the Helmholtz capacitance and the transference number [2,3]. This hopefully will stimulate discussions for the open question in the title.

### References

- [1] C. Zhang et al., *J. Phys. Energy*, **2023**, 5: 041501 [DOI: 10.1088/2515-7655/acfe9b](https://doi.org/10.1088/2515-7655/acfe9b)
- [2] C. Zhang, T. Sayer, J. Hutter and M. Sprik, *J. Phys. Energy*, **2020**, 2: 032005, [DOI: 10.1088/2515-7655/ab9d8c](https://doi.org/10.1088/2515-7655/ab9d8c)
- [3] Y. Shao, H. Gudla, J. Mindemark, D. Brandell and C. Zhang, *Acc. Chem. Res.*, **2024**, 57: 1123, [DOI: 10.1021/acs.accounts.3c00791](https://doi.org/10.1021/acs.accounts.3c00791)

# POSTER PRESENTATIONS

(ALPHABETICAL LIST)

## Electrochemical Behaviour of Selaginpulvilins

Lucie Dostálková<sup>a, b</sup>, Romana Sokolová<sup>a</sup>, Lukáš Rýček<sup>c</sup>

<sup>a</sup> J. Heyrovsky Institute of Physical Chemistry of the Czech Academy of Sciences, Dolejškova 3, 182 23 Prague, Czech Republic, lucie.dostalkova@jh-inst.cas.cz

<sup>b</sup> Charles University, Faculty of Science, Department of Analytical Chemistry, Albertov 6, 128 43 Prague, Czech Republic

<sup>c</sup> Charles University, Faculty of Science, Department of Organic Chemistry, Albertov 6, 128 43 Prague, Czech Republic

Selaginpulvilins are natural substances containing a polyarylated fluorene skeleton. These substances occur in plants of the genus *Selaginella* as their secondary metabolites and exhibit anti-inflammatory or antioxidant effects [1]. This contribution discusses synthetic derivatives of selaginpulvilins differing in the presence of a hydroxyl group (Fig.1).

Both substances were investigated using cyclic voltammetry, the hydroxylated derivative was additionally analyzed by UV-Vis spectroelectrochemistry and electrochemical impedance spectroscopy. These methods will help to propose a reaction mechanism [2-6]. Tetrabutylammonium hexafluorophosphate in a non-aqueous medium of acetonitrile was used as the supporting electrolyte, which provides a sufficiently wide potential window for studying substances oxidizing at high potentials. Both substances provided an oxidation response - the methylated derivative at potential +1.6 V, the hydroxylated derivative two oxidation waves at potentials +1.3 V and +1.6 V. The electrochemical behaviour is discussed. The electrochemical impedance spectroscopy measurement confirmed the presence of chemical step following the electron transfer.

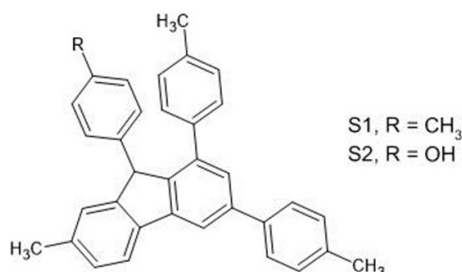


**Fig. 1:** Chemical structure of methylated (S1) and hydroxylated (S2) selaginpulvilin.

### Acknowledgement

The work has been supported by the Czech Academy of Sciences (RVO: 61388955) and Grant Agency of Charles University (project GAUK 24324).

### References

- [1] X. Liu, H. B. Luo, Y. Y. Huang, J. M. Bao, G. H. Tang, Y. Y. Chen, J. Wang, S. Yin. *Org. Lett.* 16 (2014) 282.
- [2] J. Wantulok, R. Sokolová, I. Degano, V. Kolivoška, J. E. Nycz. *Electrochim. Acta.* 370 (2021) 137674.
- [3] Š. Ramešová, I. Degano, R. Sokolová R. *J. Electroanal. Chem.* 788 (2017) 125.
- [4] H. Moreira, R. D. Levie. *J. Electroanal. Chem.* 29 (1971) 353.
- [5] D. Smith in Bard. *Electroanalytical chemistry*, New York 1970.
- [6] A. Lasia. *Electrochemical Impedance Spectroscopy and Its Application in: Modern Aspects of Electrochemistry*, Kluwer Academic/Plenum Publishers, New York 1999.

## Ion-Selective Desalination Materials

Vitali Grozovski<sup>a</sup>, Anastasiya Ivashyna<sup>a</sup>, Anita Portnova<sup>a</sup>, Jaak Nerut<sup>a</sup>, Enn Lust<sup>a</sup>

<sup>a</sup>*Institute of Chemistry, University of Tartu, Ravila 14a, Tartu, 50411 Estonia  
vitali.grozovski@ut.ee*

Desalination technology is a powerful way to lower salt concentration. It has been used to help alleviate freshwater shortages in water-scarce locations, including Africa, Asia, and the Middle East. One promising candidate to be on par with sustainability requirements is Capacitive Deionization (CDI) technology. The best CDI electrode materials require a large specific surface area, suitable pore size, hierarchical porous structure, high hydrophilicity, and high electrical conductivity [1]. This work aims to improve the conventional CDI systems by introducing the ion intercalation materials [2] to accumulate Na<sup>+</sup> and Cl<sup>-</sup> ions in the bulk of the sodium storage and chloride storage electrodes. The outcome is to provide a material with the synergistic combination of ion removal processes not only through the adsorption in the electrical double layer of the porous electrodes as in the case of classical CDI but also to add high capacity for salt removal by introducing ion intercalation materials. For this purpose, Cu-substituted, Ni- and Co-doped analogues of Prussian blue were synthesized.

The electrochemical properties of the obtained materials were studied using cyclic voltammetry in a three-electrode system in 0.1 M NaClO<sub>4</sub>, 0.1 M KClO<sub>4</sub>, and 0.1 M LiClO<sub>4</sub> aqueous solutions, focusing on the cation intercalation. The results confirmed that these Prussian Blue analogues work selectively for Na<sup>+</sup> cations. K<sup>+</sup> cations deviate from the optimal behaviour, and Li<sup>+</sup> cations cannot wholly penetrate the ion channels. It arises from the mismatch between the size of the ion channels and hydrated Li<sup>+</sup> ions (3.2 Å vs. 3.82 Å) [3]. Finally, Ni-doped Prussian blue analogue material expressed the highest activity towards Na<sup>+</sup> ion intercalation, making it suitable choice for combining with carbons with large specific surface area, appropriate pore size, and hierarchical porous structure [4-6] for hybrid CDI applications.

### References

- [1] Ying, S.; Chen, C.; Wang, J.; Lu, C.; Liu, T.; Kong, Y.; Yi, F., *ChemPlusChem*, 2021, 86 (12), 1608–1622.
- [2] Guo, J.; Wang, Y.; Cai, Y.; Zhang, H.; Li, Y.; Liu, D., *Desalination*, 2022, 528, 115622.
- [3] Qiu, S.; Xu, Y.; Wu, X.; Ji, X., *Electrochem. Energy Rev.*, 2022, 5 (2), 242–262.
- [4] R. Härmas, R. Palm, H. Kurig, L. Puusepp, T. Pfaff, T. Romann, J. Aruväli, I. Tallo, T. Thomberg, A. Jänes, E. Lust, *C-J. Carbon Res.*, 2021, 7, 29.
- [5] A. Adamson, R. Väli, M. Paalo, J. Aruväli, M. Koppel, R. Palm, E. Härk, J. Nerut, T. Romann, E. Lust, A. Jänes, *RSC Adv.*, 2020, 10, 20145–20154.
- [6] M. Härmas, R. Palm, T. Thomberg, R. Härmas, M. Koppel, M. Paalo, I. Tallo, T. Romann, A. Jänes, E. Lust, *J. Appl. Electrochem.*, 2020, 50, 15–32.

## Investigation of LTO Anodes as a Reference for EIS and NFRA Measurements

J. Jambrich<sup>a</sup>, J. Ulrich<sup>a</sup>, U. Krewer<sup>a</sup>

<sup>a</sup> Institute for Applied Materials - Electrochemical Technologies, Karlsruhe Institute of Technology, Adenauerring 20b, 76131, Karlsruhe, Germany

Extensive research efforts are currently dedicated to developing batteries with long-lasting cycling capability. For that, the ability to characterize the battery after it underwent some aging is of high importance. To study electrode kinetics and ageing in its full complexity both Electrochemical impedance spectroscopy [1] (EIS) as well as Nonlinear frequency response analysis [2] (NFRA) are adequate and powerful methods. A meaningful characterization requires measuring EIS and NFRA across varying temperatures and states of charge (SoC). To further distinguish between the effect of anode and cathode, it is vital to perform the measurements for anode and cathode separately.

Such an experimental characterization can be currently done by building experimental symmetric cells. It is very hard to achieve reliable results for SoC variability on symmetric cells, as for every SoC a different battery must be made.

This study shows how this can be circumvented by a quicker approach, which makes use of experimental cells with a  $\text{Li}_4\text{Ti}_5\text{O}_{12}$  (LTO) anode as counter electrode. LTO shows an almost constant exchange current density in the range from 10 to 90% SoC. This unique property consequently leads to SoC-independent anode spectra in the frequency range of interest. Provided that charge transfer coefficients are independent of SoC as well, the same holds for the NFR. Following, to obtain the frequency response of a single electrode for different SoCs, it is therefore sufficient to measure them on a full cell with LTO and subtract the SoC-independent anode part.

To prove the viability of the newly developed method, at first a suitable LTO electrode needed to be found. For this purpose, electrodes with aluminium as well as copper current collector were tested [1]. After that, two assumptions had to be checked: Independence of LTO spectra on SoC [2], as well as the ability to reproduce full cell spectra from spectra measured on symmetric cells (Fig 1).

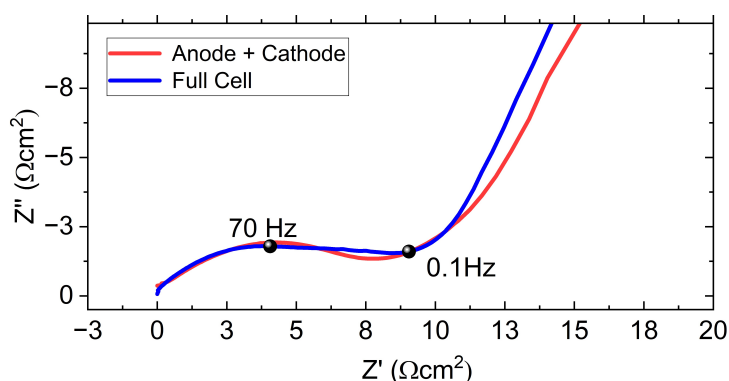


**Fig. 1:** Sum of LTO anode and NMC cathode spectra measured on symmetric cell in comparison with LTO-NMC full cell spectrum

### References

- [1] Witt, Daniel *et al.* *Batteries & Supercaps* 5.7 (2022): e202200067.
- [2] Hoon Seng Chan *et al.* *Batteries & Supercaps* 6.10, (2023), e202300203
- [3] Nina Schweikert, Horst Hahn, Sylvio Indris. *Phys. Chem. Chem. Phys.* 13 (2011), 6234-6240
- [4] Haiqing Xiao *et al.* *IOP Conf. Ser.: Earth Environ. Sci.* 474 (2020) 052038.



## Electrochemical Impedance Spectroscopy for Lithium-Ion Batteries

Kamil Jaššo<sup>a,b</sup>, Tomáš Kolenský<sup>a</sup>, Dalibor Biolek<sup>a</sup>

<sup>a</sup> Department of Electrical Engineering, Faculty of Military Technology, University of Defence, Kounicova 65, 662 10 Brno, Czech Republic

<sup>b</sup> Department of Electrical and Electronic Technology, Faculty of Electrical Engineering and Communication, Brno University of Technology, Technická 10, 616 00 Brno, Czech Republic

Among scientists, Electrochemical Impedance Spectroscopy (EIS) is often regarded as a relatively simple technique for translating complicated physicochemical phenomena into simple electrical elements. However, very often there are significant differences between scientists in using EIS and in interpreting measured impedance spectra, with EIS often seen differently by chemists than by electrical engineers and differently by theorists than practitioners. Thus, for some more complex electrochemical systems such as Li-ion batteries, there are many different equivalent circuit models (ECMs) and interpretations of the EIS [1]. This is mainly due to the fact that a single impedance spectrum can be fit by different ECMs. But how is it possible to tell which ECM is the correct one? Clearly, without a comprehensive understanding of the internal processes taking place in the measured electrochemical system, it is not possible to assign the correct equivalent electrical elements to the individual physicochemical phenomena. Despite this, many studies very often approach the measurement and evaluation of impedance spectra of Li-ion batteries without addressing their internal composition and layout, while the choice of ECM strongly depends on it and it can have a significant impact on the results. To properly select the optimal ECM, at least the basic composition of the Li-ion battery must be known.

A wide variety of different Li-ion battery ECMs have been proposed in the literature, differing in complexity, parameterization speed and accuracy. These circuits can be divided into three key categories. The first is simple Thevenin-like circuits consisting of basic ideal elements such as resistors, capacitors and inductors. These models are often used in the mathematical modeling of Li-ion batteries. For some Li-ion battery applications, such as electric vehicles or storage, these models are often sufficient. To better describe Li-ion cells and the dependence of their properties on SOC, SOH, temperature and current, more complex Randles-like circuits are used. These ECMs incorporate fictional elements such as CPE or Warburg impedance, which can better mimic real physicochemical phenomena, such as diffusion. The last category is complex ECMs for which there are several different approaches. The first approach attempts to describe the contributions of all the individual parts of a Li-ion cell by separate elements [1]. However, many physicochemical phenomena occur at similar frequencies and thus merge in the impedance spectra due to the overlap of time constants, which can lead to ambiguities in analysis. The second approach is to capture the non-linear nature of the Li-ion battery in the ECM itself, e.g. by using variable resistors, capacitors and diodes [2]. A last approach is the proposal of new unique models or elements that can better describe electrically or chemically the various processes taking place in Li-ion batteries. This work focuses on the comparison of different ECMs used to fit the measured impedance spectrum of real Li-ion batteries.

### References

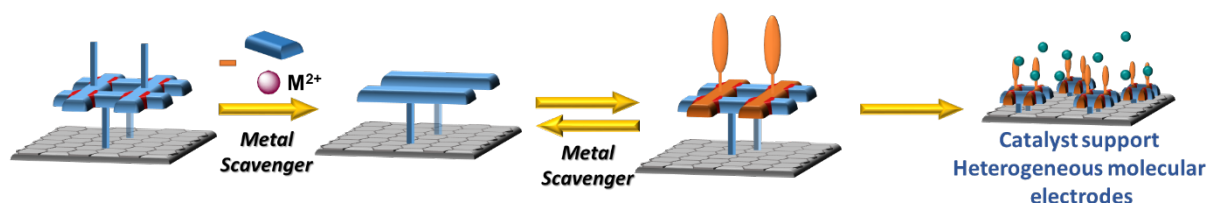
- [1] U. Westerhoff, K. Kurbach, F. Lienesch, M. Kurrat. *Energy Technol.* 4 (2016), 1620.  
 [2] J.-Y. Bae, *Batteries*, 9 (2023), 160.

## Electrochemical Characterization of Polymerized Supramolecular Grids on Electrode Surfaces

Rebeka Morvaiová<sup>a</sup>, [Alice Kulagová](#)<sup>a</sup>, Irena Hoskocová<sup>a</sup>, Jan Holub<sup>a</sup>

<sup>a</sup> Department of Inorganic chemistry, University of Chemistry and Technology, Prague, Technická 5, 166 28, Prague, Czech Republic, [kulagova@vscht.cz](mailto:kulagova@vscht.cz)

Supramolecular grids are long known class of multinuclear coordination compounds. Their main feature is a very regular rectangular shape and multicomponent constitution, which predetermines them for various applications from information storage to surface engineering. However, despite their high potential, the application reports are still lacking. This is mainly due to their tendencies to arrange in unfavourable (perpendicular to surface) configurations on surfaces [1]. Recently, a report emerged on anchoring grid-like structures on ITO electrodes through electropolymerisation [2]. Because the grids' synthesis relies on metal template self-assembly, we decided to study the nature of complexation/decomplexation processes in the electropolymerized grid and ligand films using Electrochemical Impedance Spectroscopy (EIS) in addition to standard electrochemical methods (CV, DPV). In the future, we would like to use these findings to prepare a heterofunctional grid-based layer for catalysis and sensing.



### Acknowledgement

Our group thanks the Dagmar Procházková fund (No. 101 08 2204) and the University of Chemistry and Technology, Prague, for financial support.

### References

- [1] M. Ruben, J. Rojo, F. J. Romero-Salguero, L. H. Uppadine, J.-M. Lehn. *Angew. Chem. Int. Ed. Engl.*, 43 (2004) 3644  
 [2] S. Napierała, M. Kubicki, V. Patroniak, M. Wałęsa-Chorab. *Electrochim. Acta*, 369 (2021) 137656

## LIST OF PARTICIPANTS

- Dan Bizzotto** **Prof.** ✉ bizzotto@chem.ubc.ca  
AMPEL & Department of Chemistry, University of British Columbia, 2036 Main Mall, Vancouver, BC, Canada
- Joakim Bäckström** **Assoc. Prof.** ✉ joakim.backstrom@permascand.com  
Permascand, Folkets husvägen 50, Ljungaverk, SE-84199 Sweden
- Blagoy Burdin** **Assoc. Prof.** ✉ b.burdin@iees.bas.bg  
Trakia University, Students campus, 6000 Stara Zagora, Bulgaria
- Tomáš Černoušek** **Dr.** ✉ tomas.cernousek@cvrez.cz  
Department of Material Analysis, Research Centre Řež Ltd., Hlavní 130, 250 68 Husinec-Řež, Czech Republic,
- Lucie Dostálková** **MSc.** ✉ lucie.dostalkova@jh-inst.cas.cz  
J. Heyrovský Institute of Physical Chemistry of the Czech Academy of Sciences, Dolejškova 3, CZ-18223 Prague, Czech Republic
- Shima Farhoosh** **MSc.** ✉ shima.farhoosh@fu-berlin.de  
Department of Physics, Freie Universität Berlin, Arnimallee 14, 14195 Berlin, Germany
- Miran Gaberšček** **Prof.** ✉ miran.gaberscek@ki.si  
National Institute of Chemistry, Hajdrihova 19, 1000 Ljubljana, Slovenia  
Faculty of Chemistry and Chem. Technol. University of Ljubljana, 1000 Ljubljana, Slovenia
- Vitali Grozovski** **Dr.** ✉ vitali.grozovski@ut.ee  
Institute of Chemistry, University of Tartu, Ravila 14a, Tartu, 50411 Estonia  
Department of Physical Chemistry, Eötvös Loránd University, 1117 Budapest, Hungary
- John Gustavsson** **Dr.** ✉ john.gustavsson@permascand.com  
Permascand, Folkets husvägen 50, Ljungaverk, SE-84199 Sweden
- Stanislav Hason** **Dr.** ✉ hasons@ibp.cz  
Institute of Biophysics, The Czech Academy of Sciences, Kralovopolska 2590/135, CZ-61200, Brno, Czech Republic
- Irena Hoskovcová** **Dr.** ✉ hoskovci@vscht.cz  
Department of Inorganic chemistry, University of Chemistry and Technology, Technická 5, 16628 Prague 6, Czech Republic
- Magdaléna Hromadová** **Assoc. Prof.** ✉ hromadova@jh-inst.cas.cz  
J. Heyrovský Institute of Physical Chemistry of the Czech Academy of Sciences, Dolejškova 3, CZ-18223 Prague, Czech Republic
- Jakub Jambrich** **MSc.** ✉ jakub.jambrich@kit.edu  
Institute for Applied Materials - Electrochemical Technologies, Karlsruhe Institute of Technology, Adenauerring 20b, 76131, Karlsruhe, Germany
- Kamil Jaššo** **Ing.** ✉ kamil.jasso@unob.cz

Department of Electrical Engineering, Faculty of Military Technology, University of Defence, Kounicova 65, 662 10 Brno, Czech Republic

Department of Electrical and Electronic Technology, Faculty of Electrical Engineering and Communication, Brno University of Technology, Technická 10, 616 00 Brno, Czech Republic

**Rafal Jurczakowski**

**Prof.**

✉ rafjur@chem.uw.edu.pl

University of Warsaw, Faculty of Chemistry, Laboratory of Electroanalytical Chemistry, Pasteur 1, PL-02-089, Poland

**Jana Kocábová**

**Dr.**

✉ jana.kocabova@jh-inst.cas.cz

Department of Electrochemistry at the Nanoscale, J. Heyrovský Institute of Physical Chemistry of the Czech Academy of Sciences, Dolejškova 3, 18223 Prague, Czech Republic

**Tomáš Kolenský**

**Ing.**

✉ tomas.kolensky@unob.cz

Faculty of Military Technology, University of Defence in Brno, Kounicova 65, 662 10, Brno, Czech republic

**Viliam Kolivoška**

**Dr.**

✉ viliam.kolivoska@jh-inst.cas.cz

Department of Electrochemistry at the Nanoscale, J. Heyrovský Institute of Physical Chemistry of the Czech Academy of Sciences, Dolejškova 3, 182 23 Prague, Czech Republic

**Milena Krapchanska**

**Dr.**

✉ m.krapchanska@iees.bas.bg

Institute of Electrochemistry and Energy Systems, Bulgarian Academy of Sciences, 10 Acad. G. Bonchev, 1113 Sofia, Bulgaria

Institute for Sustainable Transition and Development, Trakia University, Students Campus, 6000 Stara Zagora, Bulgaria

**Alexander Krimalowski**

**Dr.**

✉ a.krimalowski@zahner.de

Zahner-Elektrik GmbH & Co. KG, Thueringer Str. 12, 96317 Kronach, Germany

**Alice Kulagová**

**MSc.**

✉ kulagova@vscht.cz

Department of Inorganic chemistry, University of Chemistry and Technology, Technická 5, 166 28 Prague 6, Czech Republic

**Gyözö G. Láng**

**Prof.**

✉ langgyg@chem.elte.hu

Institute of Chemistry, Eötvös Loránd University, Pázmány Péter sétány 1/A, H-1117 Budapest, Hungary

**Sheena Louisia**

**Dr.**

✉ s.louisia@lic.leidenuniv.nl

Leiden institute of Chemistry, Gorlaeus Laboratories, P.O. Box 9502, 2300 RA Leiden, The Netherlands

**Jan Macák**

**Assoc. Prof.**

✉ macakj@vscht.cz

Power Engineering Department, University of Chemistry and Technology, Technická 3, 16628 Prague 6, Czech Republic

**Gábor Mészáros**

**Dr.**

✉ meszaros.gabor@ttk.hu

Institute of Materials and Environmental Chemistry, HUN-REN Research Centre for Natural Sciences, Magyar tudósok körútja 2., H-1117 Budapest, Hungary

**Nicolas Murer**

**Dr.**

✉ nicolas.murer@biologic.net

BioLogic SAS, 4 rue de Vaucanson, 38170 Seyssinet-Pariset, France

**Veronika Ostatná**

**Dr.**

✉ ostatna@ibp.cz

Department of Biophysical Chemistry and Molecular Oncology, Institute of Biophysics CAS, v.v.i., Královopolská 135, 612 00 Brno, Czech Republic

**Tamás Pajkossy** Prof. ✉ pajkossy.tamas@ttk.mta.hu  
Institute of Materials and Environmental Chemistry, Research Centre for Natural Sciences,  
H-1117 Budapest, Magyar tudósok körútja 2, Hungary

**Paolo Piccardo** Prof. ✉ paolo.piccardo@unige.it  
Department of Chemistry and Industrial Chemistry, University of Genoa, Via Dodecaneso 31, 16146  
Genoa, Italy

**Lubomír Pospíšil** Assoc. Prof. ✉ lubomir.pospisil@jh-inst.cas.cz  
J. Heyrovský Institute of Physical Chemistry of the Czech Academy of Sciences, Dolejškova 3, 18223  
Prague 8, Czech Republic

**Fermín Sáez-Pardo** MEng. ✉ fersaepa@etsii.upv.es  
IEC group, Depto. Ingeniería Química y Nuclear, Universitat Politècnica de València, Camí de Vera s/n,  
Valencia 46022, Spain

**Varsha Sasikumar** PhD. Student ✉ varsha.sasikumar@tus.ie  
Department of Electrical & Electronic Engineering, Technological University of the Shannon, Moylish  
Campus, V94 EC5T, Limerick, Ireland  
Department of Physics and Bernal Institute, University of Limerick, Castletroy, V94 T9PX, Limerick,  
Ireland

**Táňa Sebechlebská** Dr. ✉ tana.sebechlebska@uniba.sk  
Department of Physical and Theoretical chemistry, Faculty of Natural Sciences Comenius University in  
Bratislava, Mlynská dolina, Ilkovičova 6, 842 15 Bratislava, Slovakia  
Department of Electrochemistry at the Nanoscale, J. Heyrovsky Institute of Physical Chemistry of the  
Czech Academy of Sciences, Dolejškova 2155/3, 18223 Prague, Czech Republic

**Subhasis Shit** Dr. ✉ subhasis.electrochem@gmail.com  
Department of Physics, Freie Universität Berlin, Arnimallee 14, 14195 Berlin, Germany

**Romana Sokolová** Assoc. Prof. ✉ sokolova@jh-inst.cas.cz  
J. Heyrovský Institute of Physical Chemistry of the Czech Academy of Sciences, Dolejškova 3, 18223  
Prague 8, Czech Republic

**Roberto Spotorno** Prof. ✉ Roberto.Spotorno@unige.it  
Department of Chemistry and Industrial Chemistry, University of Genoa, via Dodecaneso 31, 16146,  
Genoa, Italy

**Werner Strunz** Dr. ✉ werner.strunz@zahner.de  
Zahner-Elektrik GmbH & Co KG, Thueringerstr.12, D-96317 Kronach, Germany

**Matěj Stočes** Dr. ✉ matej.stoces@metrohm.cz  
Metrohm Česká republika s.r.o., Na Harfě 935/5c, 19 000 Prague, Czech Republic

**Soma Vesztergom** Dr. ✉ soma.vesztergom@ttk.elte.hu  
Institute of Chemistry, Eötvös Loránd University, Pázmány Péter sétány 1/A, H-1117 Budapest, Hungary

**Chao Zhang** Dr. ✉ chao.zhang@kemi.uu.se  
Department of Chemistry – Ångström Laboratory, Uppsala University, Lägerhyddsvägen 1, BOX 538,  
75121, Uppsala, Sweden

## AUTHOR INDEX

	personal presentation	page
<b>Bizzotto D.</b>	Oral	11
<b>Burdin B.</b>	Oral	13
<b>Černoušek T.</b>	Oral	15
<b>Dostálková L.</b>	Poster	53
<b>Farhoosh S.</b>	Oral	16
<b>Gaberšček M.</b>	Oral	17
<b>Grozovski V.</b>	Oral and poster	18, 54
<b>Hasoň S.</b>	Oral	19
<b>Jambrich J.</b>	Poster	55
<b>Jaššo K.</b>	Poster	56
<b>Jurczakowski R.</b>	Oral	21
<b>Kolenský T.</b>	Oral	22
<b>Kolivoška V.</b>	Oral	23
<b>Krapchanska M.</b>	Oral	25
<b>Kulagová A.</b>	Poster	57
<b>Láng G. G.</b>	Oral	27
<b>Louisia S.</b>	Oral	29
<b>Macák J.</b>	Oral	30
<b>Mészáros G.</b>	Oral	32
<b>Murer N.</b>	Oral	34
<b>Ostatná V.</b>	Oral	35
<b>Pajkossy T.</b>	Oral	36
<b>Piccardo P.</b>	Oral	37
<b>Pospíšil L.</b>	Oral	38
<b>Sáez-Pardo F.</b>	Oral	39
<b>Sasikumar V.</b>	Poster	41
<b>Sebechlebská T.</b>	Oral	42
<b>Shit S.</b>	Oral	43
<b>Spotorno R.</b>	Oral	44
<b>Strunz W.</b>	Oral	46
<b>Vesztergom S.</b>	Oral	48
<b>Vladikova D.</b>	Oral	49
<b>Zhang Ch.</b>	Oral	51

# J-D-K-D QUARTET

**Jakub Janský** – violin I  
**Daniela Oerterová** – violin II  
**Karel Untermüller** – viola  
**David Havelík** – violoncello

## Program

**Johann Pachelbel:** Canon

**F. X. Richter:** Adagio and Fugue in G minor

**Wolfgang Amadeus Mozart:** Divertimento no. 1 in D major, K. 136

1. Allegro
2. Andante
3. Presto

**Antonín Dvořák:** Waltz in A major, Op. 54, no. 1

**Antonín Dvořák:** String quartet no. 12 in F major, op. 96, "American"

1. Allegro ma non troppo
2. Lento
3. Molto vivace
4. Finale. Vivace ma non troppo

Bonus:

**Astor Piazzolla:** Oblivion

---

**Antonín Dvořák (1841-1904)** composed his piano cycle *Waltzes, Op. 54* in 1879. Dvořák also arranged the first and fourth piece for string quartet. For ease of performance the second of these was transposed from the original D flat major to D major. This later quartet version of the work was only published after the composer's death, in 1911.

The String Quartet No. 12 in F major, Op. 96, nicknamed the American Quartet, is the twelfth string quartet composed by **Antonín Dvořák (1841-1904)**. It was written in 1893, during Dvořák's time in the United States. The quartet is one of the most popular in the chamber music repertoire.

## J-D-K-D QUARTET

The members of **J-D-K-D Quartet** appear regularly in Czechia in the frame of the abonnement cycles and concert tours as well as at prestigious festivals both in the Czech Republic and abroad. They are all members of the Suk chamber orchestra, one of the most prestigious ensembles in the Czech Republic.

The Suk chamber orchestra has steady cast and its first players are simultaneously soloists. The repertory includes works from baroque to contemporary music. Besides domestic concert activities the orchestra has performed in many European countries and music festivals (Prague Spring Festival, Salzburger Festspiele, Wiener Festwochen, Schleswig Holstein Festival), in the USA, Brasil, Chile, Equador, Peru, in China, South Korea and in Japan where it cooperated also with Japanese soloists, especially violinist Mariko Senju.



Violinist **Jakub Jansky**



Violinist **Daniela Oerterová**



Violinist **Karel Untermüller**



Violoncellist **David Havelík**



## GOthic CASTLE LIPNICE

The stone guardian of Sázava region, associated with the Czech writer Jaroslav Hašek, is one of the largest Czech castles, founded around 1310 by the powerful lords of Lichtemburk. In the 16th century it was converted into an imposing Late Gothic noble residence. The dilapidated castle burned down in 1869. In the 20th century after extensive archeological investigations the castle was partially renovated.



## Eavesdropping National Monument



Mouth of the truth

Bretschneider's ear



# HISTORY OF THE TOWN HAVLÍČKŮV BROD AND THE BREWERY REBEL

During the 13th century Czech inhabitants settled down in suitable places along Haberská business path that was crossing bordering woods and was connecting Czech with Moravia. One of these settlements at the bank of Sázava river was named in honour of its owner Smilův Brod (Smil's Brod).

The name of the place was later changed to Německý Brod due to the increasing number of German settlers (German Brod). At those time beer was brewed and sold there – that's the fact we are certain about.

The King Jan Lucemburský dedicated a complex of acts of grace to the contemporary owner of Německý Brod Jindřich of Lipé in 1333. This also included a contractual right to brew beer. Brewing beer was a contractual right that allowed citizens owning a house inside the town right to brew beer. This was probably for the first time when this contractual right was dedicated to a vassal town.

In 1422 the town was destroyed by the hussites. During following reconstruction were also breweries reconstructed. Consecutively all the contractual rights were certified including the right of brewing beer. Firstly by the King Jiří of Poděbrady (1452), later by the King Ludvík (1520) and the King Ferdinand (1544). In 1637 it was the last time when the Emperor Ferdinand III. claimed Havlíčkův Brod to be free regnal town and granted the town the municipal heraldry and civic rights of regnal towns.



Each citizen had originally prepared **malt and beer** himself. The citizens had also tapped beer themselves or sold it to hired inn-keepers. There were only a few houses in the town equipped completely for production of malt and beer. Therefore the citizens with the right to brew beer associated in companies that established bigger breweries. These breweries were better equipped and it was possible to prepare beer for all the citizens with contractual right to brew beer. This procedure was the same in Německý Brod.

In 1662 was a brewery near a townhall destroyed in huge fire of the town. The brewery was reconstructed in 1673 when also a guild of malsters was established. At the end of the 18th century there were two breweries in the town. One of them didn't make profit and therefore was closed down and the second brewery burnt down.



That's why the citizens bought on the 18th of October the house of Bukovský (nowadays the building of brewery restaurant Rebel), where was a little handheld brewery. This is the date of the establishment of our brewery. With increasing production of beer the capacity of the brewery couldn't be able to cope with enquiry. Therefore it was decided to reconstruct the brewery. This big reconstruction was completed on

the 12th of October 1880 when the brewery was consecrated. The production of beer was at those times 15 000 hectolitres a year.

At the turn of the 19th and the 20th century a complete equipment of the brewery was also reconstructed and in 1905 reached the most modern standard. After the rundown during the World War I. was the brewery provided with further refurbishments that influenced the production of beer. From 5320 hectolitres after the war to 30639 hectolitres in 1931. After the rundown during the World War II. production was increasing again. Name of the town was changed to Havlíčkův Brod. For almost three years was the brewery run by its owners and in 1948 was expropriated.

During the communist era was the brewery expropriated and became a part of Horácký Breweries Jihlava, Breweries of Havlíčkův Brod and East-Bohemian Breweries Hradec Králové. After the velvet revolution the brewery became again the property of the original owners. At the present the production of beer is **84 000 hectolitres a year.**

In 2004 was the own production of the malt closed down because of economic reasons. In 2008 was the situation different and malt house is after necessary repairs and investment opened again. Due to prevailing starch sources from Vysočina region gains REBEL beer protected designation Vysočina – product of the region. In 2008 was new barreling line completed and installed in production. That meant building of a new hall and a storage area for barreled beer or a workstation for dispatch department.

Brewery Havlíčkův Brod belongs to the breweries with the most modern technological equipment and in the last three years has REBEL beer become one of the most often awarded beers in Czech Republic. Brewery Havlíčkův Brod belongs to the last few independent breweries that continue in one of the oldest tradition – brewing beer.

We are proud of **protected designation České pivo** (Czech Beer) and **Vysočina regionální produkt** (The Product of Vysočina Region). Czech Beer is by Council Regulation (EC) no 510/2006 under the protection of geographical indications and designations of origin for agricultural products and foodstuffs.



*České pivo*

*(Czech Beer)*

## JAROSLAV HEYROVSKÝ (1890 – 1967)



Jaroslav Heyrovský was born on 20th December 1890 in Prague as fifth child of Leopold Heyrovský and his wife Klára, née Hanel. Both his father and grandfather were lawyers; however, young Jaroslav did not show any interest in that family line. From his early childhood he was attracted by natural objects, mineral, botanical and animal.

In 1904 the recently introduced Nobel Prize for chemistry was awarded to the English physical chemist William Ramsay for his discovery and isolation of the rare gas elements. Jaroslav became inspired by the Ramsay's experiments, described in the press, to that extent, that he firmly decided he must become physical chemist. After maturity examination in 1909 he registered at the Faculty of Philosophy of the Prague University for the study of physics, mathematics and chemistry. During the first year at the university he discovered that there was no special subject of physical chemistry, and he begged his father to allow him to continue his studies at the London University College where William Ramsay was teaching. There he still could attend Ramsay's lectures until 1913, when the great scientist retired. In his position at University College Ramsay was followed by professor F.G.Donnan, who was specialized in electrochemistry. Jaroslav, who in that year gained the title Bachelor of Science (BSc), became Donnan's demonstrator for the year 1913-14, which decided about his orientation towards electrochemistry.

The intensive work in that direction was interrupted in 1914 by the outbreak of the First World War, after the student went home for summer holidays. Instead of returning to London he was enrolled in the Austro-Hungarian army to serve as dispensing chemist and radiologist in military hospitals.

After the end of the war, he was able to pass doctorate examinations and to defend his PhD thesis at the Prague University.

The examination in physics was conducted by professor Bohumil Kučera, author of the method of measuring



surface tension of polarized mercury by weighing drops of mercury from dropping mercury electrode. Next day after the examination Heyrovský visited Kučera's laboratory to get acquainted with his experimental set-up and the satisfied professor advised the student to continue in research of the method. Heyrovský replaced collecting, counting, drying and weighing the drops of mercury by measuring the drop-time, which is also proportional to surface tension. He found that from electrocapillary curves the values of "decomposition voltage" of compounds of various metals could be determined. Of these results he lectured at a meeting of the

Union of Czech Mathematicians and Physicists in spring 1921, still in presence of professor Kučera, who shortly after that passed away prematurely.

In order to gain more electrochemical data about the dropping mercury electrode system Heyrovský decided to measure, besides the drop-time, also **the current passing through the mercury drops at each value of applied voltage**. The first measurement of this kind was done on 10th February 1922 and it came out, that from the thus gained current / voltage curve one can determine both quality and quantity of substances dissolved in the solution into which the electrode drops. That day can be hence considered as the birthday of polarography, although the term „polarography“ was coined later. The work on electrolysis with dropping mercury electrode was published first in Czech in 1922 by Chemické Listy, an enlarged English version appeared one year later in Philosophical Magazine.

Aware of the disadvantage of the time-consuming manual recording of the curves point-by-point, Heyrovský together with M. Shikata from Japan (who joined him to learn about this new method) suggested automation of the method with photographic recording of the curves. For the automatic instrument they introduced the term “polarograph”, i.e., apparatus drawing course of electrochemical polarization.

Since 1922 Heyrovský was director of the newly established Department of physical chemistry, in 1926 he became full professor of that subject, first at Charles University. He had many students and coworkers from Czechoslovakia as well as from abroad (Wiktor Kemula from Poland, from Italy Giovanni Semerano, from USSR Emilia Varasova, from USA O. H. Müller, from France Edgar Verdier etc.).



After the 2<sup>nd</sup> World War in Czechoslovakia a specialized Polarographic Institute was founded in April 1950 under directorship of Jaroslav Heyrovský. Today's the J. Heyrovský Institute of Physical Chemistry of Academy of Sciences of the Czech Republic is its direct follower.

Heyrovský himself was lecturing on polarography in many countries. Since 1934 he was repeatedly suggested for Nobel Prize for the discovery and development of polarography, finally in 1959 several simultaneous proposals were accepted, and in December that year the Swedish king transmitted the **Nobel prize for chemistry to Heyrovský** in Stockholm (foto). In that way Jaroslav Heyrovský's whole life's dedicated work got its highest appreciation.

He died in Prague on March 27th 1967. (Until now, he is the only Czech who received this prize for sciences; the second Czech Nobel prize winner was Jaroslav Seifert, poet, for literature.)

## 55 YEARS OF HEYROVSKÝ DISCUSSION MEETINGS (1967 – 2024)

Since 1967 his pupils and followers organise every year a small international meeting, called Heyrovský Discussion. The purpose of the Discussions is to bring together, on invitation by the Organizing Committee, a limited group of specialists in a particular field of electrochemistry, and to enable them to exchange ideas and views on their research problems in an informal and friendly atmosphere. This was the way how polarography was developing under the guidance of Professor Heyrovský between the I. and II. world wars at Charles University in Prague; hence the name of this scientific gathering. Every year a different subject has been selected for the Discussion. The theme of electrochemistry of organic, organometallic and coordination compounds (Molecular electrochemistry) has been discussed in last decades eight times (bold in the list below).

The following topics were discussed so far:

- 1967 Adsorption at Electrodes and its Influence upon Electrode Processes
- 1968 Adsorption and Processes on Catalytic Electrodes
- 1969 Mechanism of Redox Reaction Proper
- 1970 Intermediates and Products of Electrode Reactions
- 1971 Products and Intermediates of Redox Reactions
- 1972 New Principles in Electroanalytical Chemistry
- 1973 Deposition and Oxidation of Metals
- 1974 Electrochemistry in Non-Aqueous Solvents
- 1975 Electrochemical Phenomena in Biological Systems
- 1976 Redox Reactions of Coordination Compounds
- 1977 New Horizons in Polarography
- 1978 Electrochemical Energy Conversion
- 1979 Electrochemistry in Environmental Protection
- 1980 Electrochemical Phenomena on Membranes and Biomembranes
- 1981 Fundamentals of Preparative Organic Electrolysis
- 1982 New Principles in Electroanalysis
- 1983 Photochemical Stimulation of Redox Reactions
- 1984 Electrochemical Processes in Two-Phase Liquid, Microemulsion and Micellar Systems
- 1985 Recent Aspects of Electrocatalysis
- 1986 New Aspects of Electrochemical Materials Fundamentals

- 1987 Ecoelectrochemistry general
- 1988 Electrochemistry of Separation and Synthetic Processes at Liquid/Liquid Interfaces
- 1989 Catalytic Homogeneous Processes Combined with Electrochemical Charge or Group Transfer
- 1990 Electrochemistry on Organized Molecular and Polymolecular Structures
- 1992 Electroanalysis and the Environment
- 1993 Progress in Organic and Organometallic Electrochemistry
- 1994 Electrochemical Processes on Liquid Membranes
- 1995 Electrochemistry of Biologically Active Compounds and Their Models
- 1996 Advanced Techniques in Electrochemistry
- 1997 Electrochemistry at Liquid/Liquid Interface
- 1998 Electrochemistry for Analytical Separations
- 1999 Organic Electrochemistry
- 2000 Nanostructures on Electrodes
- 2001 Chemistry on Polarised Liquid-Liquid Interfaces
- 2002 Electrochemical Impedance Analysis**
- 2003 Electrochemistry of Biological Systems and Their Models
- 2004 Applications and Methodologies in Electrochemistry on Liquid-Liquid Interfaces
- 2005 Electrocatalysis in Nanoscale
- 2006 Electrochemical Impedance Analysis**
- 2007 Electrochemistry of molecules with multiple redox centers
- 2008 Electrochemical Impedance Spectroscopy**
- 2009 Liquid-liquid Electrochemistry - from Fundamentals to Applications
- 2010 Electrochemistry of Organic Molecules and Coordination Compounds
- 2011 Nanostructures on Electrodes
- 2012 Electrochemistry of Biopolymers and Bioactive Compounds
- 2013 Molecular Electrochemistry in Organometallic Science
- 2014 Electrochemistry of Organic and Bioactive Compounds
- 2015 Progress in Electrochemistry at Liquid-liquid Interfaces and Liquid Membranes
- 2016 Electrochemical Interfaces at the Nanoscale
- 2017 Molecular Electrochemistry in Organic and Organometallic Research
- 2018 2D and 1D Materials
- 2019 Electrochemical Investigation of Organic Compounds and Biopolymers
- 2020 Rational Electrocatalysis
- 2023 Molecular Photo-spectroelectrochemistry, Mechanisms and Electrosynthesis
- 2024 Electrochemical Impedance Analysis**

# HISTORY OF THE CASTLE TŘEŠŤ AND OF THE TOWN

In the heart of Czech-Moravian Highland, nearly at the halfway between Prague and Vienna, in the hill pass, the town of Třešť is situated. The parish village Třešť was founded during the colonization of the Czech-Moravian deep forest in the course of the 13th century at the crossroads of two historical trade routes. The first written record about Třešť comes from 1349, when the parish church is reminded. Jewish community appeared quite early in Třešť; there are some references about a rabbi Jakub from Třešť even from the second half of 13th century. The Jewish population in Třešť was 621 people in 1845 but the number was falling and, in 1930, only 64 Jewish citizens remained in Třešť. They became the victims of holocaust.

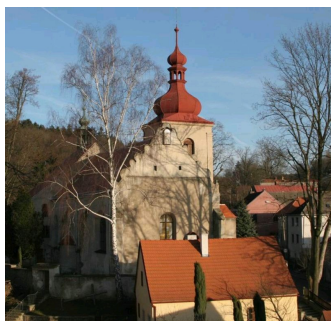
In the town, many handicrafts were developing and guilds were flourishing. In 19th century, the cloth making factories, furniture plants (producing especially carved clock cabinets exported all around Europe) and matches industry was gradually emerging.



## **The former aristocrat mansion,**

nowadays a castle hotel went through a rich development. It stands on the place of the medieval citadel from 12th century. Starting from 1513 the castle was rebuilt in the renaissance style: a four-wing building with corner towers and arcades was constructed. After 1945, the castle turned into a municipal museum and a gallery. Together with

the adjoining park (15 ha) it became the property of the Academy of Science of the Czech Republic in 1984. After ten years of intensive restoration works, the castle was transformed into a conference centre in 1994.



## **The parish church of St. Martin**

It is the oldest monument in the town. It was founded in the 13th century, completed in the second half of the 15th century and later baroquized. We can notice a Gothic tombstone, a stone late Gothic pulpit and a Renaissance Kryštof Vencelík's tombstone.

## **The church of St. Catherine Siens**

is also a remarkable point of interest. It was founded in the 16th century, in times when Třešť belonged to the Venclík family. The presbytery was rebuilt in the 18th century, the inside furnishing of the church is from the 19th century (the restoration after the fire in 1824). There are two late Renaissance tombstones: of J. V. Venclík from Vrchoviště on the outside plaster from 1616 and an unknown knight with the coat of arms where a half-lion is pictured.



## **Former Jewish Synagogue**



An Empire synagogue was constructed after a great fire (2nd October 1824) which destroyed all the Jewish ghetto. It was restored and consecrated on 22nd September 1825. On the ground floor facing the street an arcade is its typical feature. Nowadays the synagogue serves as a church of Czechoslovak Hussite Church. You can visit there an exhibition with many documents describing the history of Třešť Jewish community.



